UNIVERSIDADE DA BEIRA INTERIOR
Ciências da Saúde

Purification of DNA vaccine to prevent or treat cervical cancer

Ana Rita Santos Simões

Dissertação para obtenção do Grau de Mestre em
Ciências Biomédicas
(2º ciclo de estudos)

Orientadora: Profª. Doutora Ângela Sousa
Co-orientadora: Profª. Doutora Diana Costa

Covilhã, Outubro de 2016

Acknowledgements

I wish to thank all of those who contributed to the fulfilment of this work, directly or indirectly.

First, a special thank you to my supervisor Professor Doctor Ângela Sousa for all the guidance, support and help that you gave me throughout this year. Without your valuable knowledge and belief in me, this work would not have been possible.

To my co-supervisor Professor Doctor Diana Costa, for the shared knowledge and suggestions, for the constant availability. Thank you for always being patient and encouraging me.

To the University of Beira Interior, particularly to the Health Sciences Research Centre, where the entire research project was developed.

To my lab colleagues, especially Margarida Almeida, for your constant help, availability and patience at any time over the entire year, for sharing the knowledge that made me able to accomplish this work and for always answering my questions.

To Patrícia Pereira and Joana Tomás, for helping me on the last stage of my work. Your advice was essential to obtain some of the results.

To Engª Ana Paula for accompanying me during the acquisition of SEM and TEM images, and to Catarina Ferreira for accompanying me during the Confocal Microscopy visits.

To my dear friends who were always there for me, for all the talks, the coffees and the laughs.

I am also extremely grateful to my family, my parents and brother, for giving me the chance to grow professionally and personally and for always believing in me. You make me the person I am today. For all your love, support and advice, a very big thank you.

To my boyfriend André for all the patience and support you give me every day. You give me the strength to never give up and even far away you are always there for me. Thank you for making me smile.

Resumo alargado

A infeção causada pelo Vírus do Papiloma Humano (HPV) é uma doença sexualmente transmitida, que afeta tanto homens como mulheres a nível mundial. Em último caso, a infeção causada pelo HPV pode levar ao aparecimento de massas tumorais. De facto, o ácido desoxirribonucleico (DNA) do HPV foi encontrado em 99,7% dos casos de cancro do colo do útero, provocando mais de meio milhão de mortes. A progressão do cancro é devida à expressão das oncoproteínas E6 e E7, consideradas tumorogénicas pela sua capacidade de alterar o ciclo celular, sendo estas responsáveis pela replicação viral e transformação e imortalização das células hospedeiras. Atualmente, existem apenas duas vacinas comercializadas contra a infeção pelo HPV: a Gardasil® e a Cervarix®. Estas vacinas profiláticas ativam unicamente a imunidade humoral, pela geração de anticorpos contra o HPV e são somente preventivas, ou seja, apenas são efetivas antes de ocorrer a infeção. Assim, as vacinas terapêuticas têm a promissora vantagem de conseguir eliminar lesões pré-existentes e até tumores.

Surgem então algumas estratégias terapêuticas inovadoras, como a terapia génica e as vacinas de DNA, que ativam tanto a resposta humoral como a celular, permitindo a prevenção e o tratamento de doenças como o cancro do colo do útero. Nas vacinas de DNA, o uso do DNA plasmídico (pDNA) como vetor não viral torna-se bastante apelativo, não só pela sua baixa toxicidade e elevada segurança, mas também pela simples produção e aplicação. A produção destas vacinas requer a purificação à escala preparativa do pDNA superenrolado (sc), considerada a isoforma biologicamente ativa. É, por isso, necessário explorar diversas estratégias de purificação de forma a obter o maior rendimento e pureza do pDNA sc.

A cromatografia de afinidade com aminoácidos tem demonstrado ser uma abordagem promissora, pois permite a interação seletiva entre ligandos específicos e as biomoléculas de interesse, à semelhança de interações biológicas que ocorrem naturalmente entre proteínas a aminoácidos no organismo. Para além disso, o uso de monolitos como suporte cromatográfico tem vindo a demonstrar que estes suportes são uma excelente alternativa aos convencionais, visto terem uma maior capacidade de ligação para moléculas de grandes dimensões e que possibilitam a utilização de fluxos mais elevados, diminuindo o tempo de retenção da biomolécula de interesse, evitando assim a sua degradação.

Assim, o presente trabalho teve como primeiro objetivo explorar diferentes estratégias de eluição cromatográficas, utilizando um monolito de arginina com um braço espaçador, no sentido de purificar o pDNA sc a usar numa vacina de DNA contra o cancro do colo do útero. Inicialmente, foram realizados vários ensaios, quer em condições de eluição iónicas quer hidrofóbicas, para avaliar o comportamento cromatográfico e a influência dos diferentes grupos imobilizados no monolito de epóxi. Depois, o monolito de arginina com um braço

espaçador foi caracterizado em termos de capacidade dinâmica de ligação (2.53 mg/mL obtido a 10% da curva "breakthrough"), confirmando que este suporte apresenta maior capacidade de ligação do que um suporte convencional (0.133 mg/mL), modificados com o mesmo ligando (arginina). Por outro lado, este valor é menor que o valor de capacidade de ligação obtido com o monolito de arginina (3.55 mg/mL), provavelmente devido à eletronegatividade do braço espaçador que promove repulsão pelo pDNA. Para avaliar a seletividade do suporte, vários ensaios foram realizados utilizando amostras de plasmídeo pré-purificado com o *kit* comercial (isoformas circular aberta, linear e sc), manipulando a concentração de cloreto de sódio (NaCl) e o pH do tampão de eluição. Os resultados comprovaram que é possível obter a isoforma sc purificada, apesar da sua recuperação ser ligeiramente sacrificada. Posteriormente, prosseguiu-se para a purificação do pDNA sc a partir de uma amostra mais complexa de lisado de *Escherichia coli* (*E. coli*). Diferentes estratégias de eluição foram abordadas, incluindo a manipulação de NaCl e pH, assim como a adição de arginina no tampão de eluição como agente de competição. Após várias otimizações, a estratégia que melhor resultou na purificação da isoforma de interesse foi a de um gradiente por passos com o tampão de equilíbrio a 680 mM de NaCl em tampão 10 mM tris e 10 mM EDTA (Tris-EDTA), pH 7 e o tampão de eluição a 649 mM e 1 M de NaCl em Tris-EDTA, pH 7,5. Esta estratégia cromatográfica permitiu obter o plasmídeo sc com 93,3% de pureza e 72% de recuperação. A aplicabilidade do monolito de arginina com um braço espaçador na purificação do plasmídeo à escala preparativa também foi avaliada, tendo-se recuperado o plasmídeo com 98,5% de pureza. As impurezas (DNA genómico, proteínas e endotoxinas) das frações recolhidas de pDNA sc, tanto na escala laboratorial como na preparativa, foram quantificadas, estando os resultados dentro dos valores recomendados pelas agências reguladoras. Assim sendo, o monolito de arginina com um braço espaçador permitiu uma rápida e eficaz separação do pDNA sc, recorrendo a baixas concentrações de sal, tanto numa escala laboratorial como preparativa.

Por outro lado, sabe-se que apenas um em mil plasmídeos apresentados às células eucarióticas conseguem alcançar o núcleo e levar à expressão do gene de interesse. Desta forma, torna-se crucial desenvolver estratégias que permitam a proteção do pDNA e que facilitem a sua entrada no núcleo. O uso de nanopartículas tem revelado ser uma valiosa solução, pois além de protegerem o pDNA da degradação enzimática, permitem uma entrega específica e, consequentemente, um aumento na transfeção celular. Assim sendo, este trabalho teve como segundo objetivo a formulação de nanopartículas de carbonato de magnésio ($MgCO_3$) e gelatina, funcionalizadas com os ligandos de manose e galactose para direcionar as nanopartículas para as células alvo (células dendríticas). Em termos da morfologia, as imagens obtidas na microscopia eletrónica de varrimento (SEM) e na microscopia eletrónica de transmissão (TEM) permitiram concluir que todos os sistemas adquirem uma forma arredondada. Foi também calculada a eficiência de encapsulação (EE) dos diferentes sistemas com diferentes quantidades de pDNA, constatando-se que o sistema

com 5 µg de pDNA possibilitou uma melhor encapsulação (cerca de 87%). Para além disso, a gelatina permitiu diminuir o tamanho médio das nanopartículas e a funcionalização com os ligandos de manose e galactose não aumentou significativamente o tamanho das nanopartículas de gelatina, estando os valores entre 99,7 nm e 237,4 nm. Por fim, os valores do potencial zeta foram positivos, o que sugere uma interação facilitada das nanopartículas com a membrana celular que é carregada negativamente, possibilitando uma transfeção mais eficiente. Todos os sistemas estudados apresentam características promissoras para um *uptake* celular adequado, o que foi comprovado pela transfecção de células *HeLa*.

Em conclusão, o presente trabalho mostrou que o monolito de arginina com braço espaçador permitiu a purificação do pDNA sc com um bom grau de pureza e recuperação e as nanopartículas de $MgCO_3$ provaram ser um sistema de entrega eficiente, sendo uma estratégia promissora para o desenvolvimento de uma vacina de DNA eficaz contra infeções provocadas pelo HPV.

Palavras-chave

Cromatografia de afinidade; HPV; $MgCO_3$; Monolito de arginina com braço espaçador; Nanopartículas; Plasmídeo superenrolado; Vacina de DNA plasmídico.

Abstract

Human Papillomavirus (HPV) is worldwide sexually transmitted and associated with 99.7% of cervical cancer. The cancer progression is due to the expression of the oncoproteins E6 and E7, which can alter the cell cycle and are responsible for the viral replication and transformation of host cells. The vaccines available are only preventive ones, it being necessary to develop therapeutic ones, to prevent and treat a pre-existent infection.

Deoxyribonucleic acid (DNA) vaccination along with the use of plasmid DNA (pDNA) as a non-viral vector arises as a good strategy that can activate both humoral and cellular immune responses, allowing the prevention and treatment of HPV infections. The combination of the amino-acid affinity chromatography (AC) with the innovative monolithic supports appears as a promising approach to obtain highly purified supercoiled (sc) pDNA – the active biological conformation – with high purity and recovery. This allows the selective interaction of specific ligands to the target biomolecule adding to the higher capacity of monoliths when compared to conventional chromatographic supports. Monoliths also allow the use of high flow rates, which allows a fast purification procedure and decreases the retention time of the target biomolecule, avoiding its degradation. In the present work, different elution strategies (manipulation of sodium chloride (NaCl) concentrations and/or pH and competition) were explored, in order to purify the supercoiled HPV-16 E6/E7^{MUT} pDNA, by using the arginine monolith with spacer arm. The best elution strategy applied on both laboratorial and preparative scales allowed the removal of impurities within the regulatory agency recommendations, with 93.3% and 98.5% of purity degree, respectively. This reinforces the applicability of this monolith for the sc pDNA purification.

Moreover, only one in thousands naked plasmids presented to the cells reach the nucleus and are expressed. The use of nanoparticles is a valuable strategy that permits the protection of the pDNA by avoiding the enzymatic degradation and facilitates the specific delivery, enhancing the cellular transfection. Thus, different magnesium carbonate ($MgCO_3$) systems were characterized regarding its encapsulation efficiency (around 87%), morphology (round shape), size (99.7-237.4 nm) and zeta potential (positive). These data suggest that the developed nanoparticles are suitable for cellular uptake and thus appropriate for therapeutic applications. Additionally, *in vitro* studies accompanied with confocal microscopy were performed, which revealed that all the formulated systems are able to transfect eukaryotic cells.

Keywords

Affinity chromatography; Arginine monolith with spacer arm; DNA vaccine; HPV infection; $MgCO_3$ nanoparticles; Supercoiled plasmid DNA.

Table of contents

List of Figures

Chapter I - Introduction

Chapter II -Materials and methods

Chapter IV - Results and discussion

List of Tables

Chapter I - Introduction

Chapter IV - Results and discussion

List of Acronyms

AC	Affinity chromatography
AIDS	Acquired immunodeficiency syndrome
AP 1	Activator protein 1
APC	Antigen-presenting cell
ATPase	Adenosine triphosphatase
bp	Base pairs
BCA	Bicinchoninic acid
BSA	Bovine Serum Albumin
ºC	Celsius
$CaCO_3$	calcium carbonate
cccDNA	Covalently closed circular DNA
CO_2	Carbon dioxide
Cys	Cysteines
CR	Conserved Regions
CT	Control
DBC	Dynamic binding capacity
DC	Dendritic cell
DNA	Desoxirribonucleic acid
E6AP	E6-associated protein
E. coli	*Escherichia coli*
EDTA	Ethylene-diamine tetraacetic acid
EMEA	European Agency for the Evaluation of Medical Products
EU	Endotoxin units
FBS	Fetal bovine serum
FDA	Food and Drug Administration
FITC	Fluorescein isothiocyanate isomer I
g	Gram
gDNA	Genomic DNA
Glu	Gluteine
h	Hour
HCl	Chloride acid
HPV	Human Papillomavirus
Kbp	kilo base pairs
KDa	Kilo Dalton
KH_2PO_4	Monopotassium phosphate
K_2HPO_4	Dipotassium phosphate
KRF 1	Keratinocyte-specific transcriptional factor 1

Kv	Kilovolt
LAL	Limulus amebocyte lysate
LCR	Long control region
Leu	Leucine
M	Molar
mAU	Miliabsorbance units
$MgCl_2$	Magnesium chloride
$MgCO_3$	Magnesium carbonate
MHC	Major histocompatibility complex
min	Minute
mL	Milliliter
mM	Millimolar
MTT	3-[4,5-dimethyl-thiazol-2-yl]-2,5-diphenyltetrazolium bromide
NaCl	Sodium chloride
$NaCO_3$	Sodium carbonate
NaOH	Sodium hydroxide
NF-I/CTF	Nuclear factor
nm	Nanometer
oc	Open circular
OD_{600}	Optical density at 600 nm
ORF	Open reading frame
PBS	Phosphate buffered saline
PCR	Polymerase chain reaction
pDNA	Plasmid DNA
pRb	Retinoblastoma protein
RNA	Ribonucleic acid
rpm	Revolutions per minute
sc	Supercoiled
SD	Standard deviation
SDS	Sodium dodecylsulfate
SEM	Scanning electron microscopy
TAE	Tris, acetic acid, EDTA
TEM	Transmission electron microscopy
Tris	Tris(hydroxymethyl) aminomethane
Tris-EDTA	10 mM Tris-HCl and 10 mM EDTA
UV	Ultraviolet
v:v	Volume:volume
w/w	Mass/mass
µg	Microgram
µL	Microliter
µm	Micrometer

Chapter I – Introduction

1.1 Human Papillomavirus

HPV infection is a widespread and most common sexually transmitted disease, that affects both women and men [1]. Even though the risk of this infection remains during a woman's lifetime, it is often acquired by adolescents and young adults, especially in ages between 15 and 19 years old [2]. It can infect the anogenital region and other mucosal sites of the body and it can lead to vulvar/vaginal precancerous lesions, genital warts and respiratory papillomatosis and also different kinds of cancer, such as vulvar, vaginal, anal, penile or cervical cancer [2, 3]. This last one represents the second largest cause of cancer death of women worldwide. In fact, the HPV DNA has been found in 99.7% of cervical cancer, being the most common cause of mortality by this type of cancer – more than half a million cases, 270.000 ending with death [4, 5]. Furthermore, recent studies suggest that this type of infection might also affect fertility and change the efficacy of assisted reproductive technologies [1]. As listed before, HPV infections cause a large spectrum of epithelial lesions. This happens because there are more than 150 different HPV types that have been already identified based on DNA sequence analysis and each is associated with an infection at a specific epithelial site [1, 3]. Of these, more than 30 cause cervical epithelium lesions and some of these lesions can ultimately lead to cancer [6].

HPVs belong to *Papovaviridae* family [7]. They are divided into several groups or genera. The two main ones are the *Alpha* and the *Beta* Papillomaviruses. *Beta* Papillomaviruses are normally associated to cutaneous infections and *Alpha* Papillomaviruses are associated to genital/mucosal infections and they represent the largest group of HPVs. Some *Alpha* HPVs, such as HPV-2, can also include some cutaneous lesions, like common skin warts and are hardly ever related to cancer [6, 7]. According to their tendency to cause cervical cancer, this group is then subdivided into those that have low risk, intermediate risk and high risk [8]. Inside the high risk group, also called oncogenic group, HPV-16 is the most prevalent one and is responsible for nearly 60% of cervical cancer and HPV-18 is the second most common, causing 10-20% of this type of cancer [3, 9]. The low risk type of HPVs usually causes genital warts and it almost never progresses to cancer. The HPVs that belong to the other genera cause mostly cutaneous papillomas and verrucas, but not any type of cancer [3]. Seeing that HPV can induce a diversity of lesions and cancers and it is the responsible for the majority of cervical cancers, it has been studied increasingly and so have been the ways to prevent and treat his consequences, like vaccination.

1.1.1 HPV structure and genome organization

HPV is small, with approximately 55 nm in diameter, does not have any envelope and has an icosahedral capsid composed of 72 capsomers. His DNA is double-stranded and circular, with

around 8000 base pairs (bp) [10, 11]. HPV genome is divided into three main regions: the long control region (LCR), that covers about 10% of the genome, the region of the early genes, over 50% of the genome, and the region of the late genes, almost 40% of the genome (figure 1) [12] . These two last regions are generally called open reading frames (ORFs) [10].

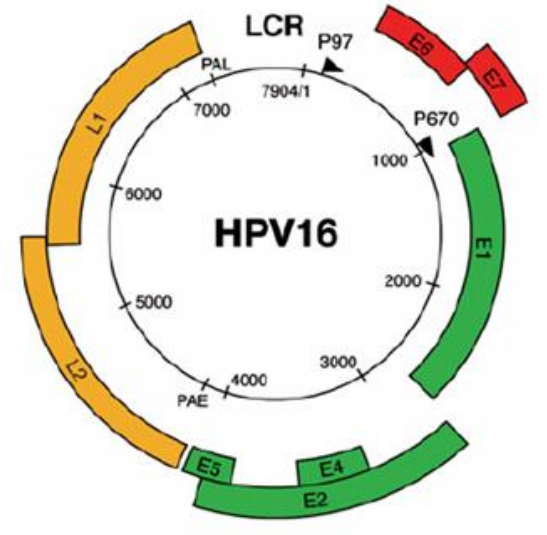

Figure 1 - Genome and structural organization of the HPV-16. The HPV-16 genome is represented as a black circle with the early (p97) and late (p670) promoters marked by arrows. The early genes (E1, E2, E4 and E5) are represented in green and the early genes (E6 and E7) in red. The late genes (L1 and L2) are represented in yellow. The LCR is presented between yellow and red regions [6].

The LCR is a segment of about 850 bp next to the origin of viral replication. This part of the genome does not encode any protein, but despite that it is also relevant since it has several binding sites for a lot of different transcriptional repressors and activators, including the activator protein 1 (AP1), the keratinocytic-specific transcription factor 1 (KRF l), nuclear factor (NF-I/CTF) and some viral transcriptional factor that are encoded by the early region. For this reason, the LCR regulates the transcription of the early and late regions, hence it controls the expression of viral proteins and infectious particles. The host range of specific HPV types is quite determined by LCR, since it has the capacity for binding so many transcription factors [11].

The segments of the genome that actually encode proteins are called ORFs. The late gene region has two of this ORF and encodes for two proteins: the L1 protein and the L2 protein. These two proteins are the structural components that form the viral capsid and are only expressed in productive infected cells [10, 13]. The L1 protein is the major viral capsid protein and is highly conserved through the different Papillomavirus species. In turn, the L2 protein is the minor viral capsid protein and has much more sequence variation amongst HPV types than the L1 protein [11]. Their expression is tightly regulated and linked to the differentiation of infected epithelial cells [4].

The early gene region encodes for viral replication and cellular transformation and it consists of six ORFs: the E1, E2, E4, E5, E6 and E7 (table 1) [10, 12]. Depending on the HPV type, the E4, E5 and E7 genes usually encode for a single polypeptide, while the E1, E2 and E6 genes can suffer different splicing and so be expressed as several related polyproteins [14].

The E1 gene is expressed in 68 and 27 kDa polypeptides. The 68 kDa protein has adenosine triphosphatase (ATPase) and helicase activities and it can bind to specific sequences within the LCR so the DNA replication starts [14]. The HPV E2 gene encodes for two proteins that, along with E1, are necessary for extrachromosomal DNA replication [11]. The E2 proteins have from 370 to 430 amino acids in length and DNA binding domains, that can function as transcriptional activators or repressors – they are the major regulator in virus transcription and genome replication [14].

The HPV E4 protein seems to have an important role on the maturation, replication of the virus and the release on the HPV particles and, like the L1 and L2 capsid proteins, it is only expressed in later stages of the infection, at the assembly of the complete virions [11, 14]. Apparently, this protein does not transform the cells, but it can associate with cellular membranes and accumulate in the cytoplasm, inducing the collapse of the cytoplasmic cytokeratin network, in human keratinocytes, promoting the necessary conditions to the release of the virions [15].

The HPV E5 is a small polypeptide with highly conserved 44-80 amino acids [14]. Usually, the E5 gene is not expressed in cervical carcinoma cells, suggesting that is not essential in the malignant transformation of the host cell and thus its exact role in human cancers is yet to be known. Despite this, it is already established that E5 interacts with cell membrane receptors, like epidermal growth factor, platelet-derived growth factor ß and colony stimulating factor, stimulating the cell proliferation of HPV infected cells [11, 15].

Lastly, the E6 and E7 genes express two oncoproteins indispensable for the viral replication and the host cell immortalization and transformation [15]. These are pleiotropic proteins, since they can make transmembrane signaling, regulate cell cycle, immortalize primary cell line and regulate chromosomal stability [16].

These two proteins are considered tumorigenic, because they have the capacity to bind to some tumor suppressor proteins, like p53 and retinoblastoma protein (pRb), consequently preventing the HPV infected cell's apoptosis and enhancing their malignant conversion [13]. The function of E6 and E7 will be detailed in next chapters.

Table 1 - A summary of the HPV ORFs (adapted from [14]).

Viral protein	Function
L1	Major capsid protein
L2	Minor capsid protein
E1	Viral DNA synthesis
E2	Transcription regulation
E4	Disrupts cytokeratins, late protein
E5	Interacts with growth factor receptors
E6	Transforming protein; binds and initiates p53 degradation
E7	Major transforming protein; binds pRb, p103 and p107

1.1.1.1 E6 oncoprotein

The E6 protein has approximately 150 amino acid residues and 18 kDa and it can be found in the nuclear matrix and other nonnuclear membranes [17, 18]. E6 and E7 proteins bind to zinc ion through the coordination of cysteine residues [19]. The E6 contains four Cys-X-X-Cys motifs that form two zinc-binding domains, joined by an interdomain linker of 36 amino acids [19, 20]. E3 ubiquitin ligase, also known as E6 associated protein (E6AP), forms a complex with both E6 and some target proteins. The motif through which there is a binding between E6, E6AP and the target proteins is referred to as LXXLL motif and is conserved throughout the E6 proteins of numerous Papillomaviruses. Another motif that all high risk E6 proteins have is referred to as XT/SXV and it is responsible for the binding to specific domains on cellular proteins that are known as PDZ proteins. Some other proteins, namely p53, Bak and procaspase 8, do not have the LXXLL nor the PDZ domain, nevertheless they bind to E6 protein, possibly through other yet undefined motifs or indirectly through binding to E6AP or other E6 associated proteins. As mentioned above, the E6 protein can interact with a wide number of target proteins, but the most well studied E6-protein interaction is with the p53 tumor suppressor protein [19].

p53 is a nuclear protein that functions as a transcriptional factor and regulates the transcription of various downstream target genes, which controls cell cycle arrest, apoptosis, DNA repair, senescence and metabolism [21]. The increase of p53 is triggered by cellular damage and it activates pathways for DNA repairs, cell arrest and/or apoptosis [19]. When there is damage in the DNA, p53 induces cell growth arrest in the G1 phase of the cell cycle, so it can be repaired. This is important for the genomic integrity maintenance [11].

Therefore, by targeting p53 for degradation and so interfering with its biological function, E6 promotes cell transformation and proliferation. This degradation occurs via the formation of the complex that includes p53, E6 and E6AP, causing the transfer of ubiquitin peptides to p53, which marks it for degradation by a proteasome. Low risk HPV E6 cannot target p53 for degradation by the proteasome as it happens with the high risk HPV E6. In this way, the E6 disturbs the control of the cell cycle progression, leading to an increase of tumor cell growth at the end (figure 2) [16].

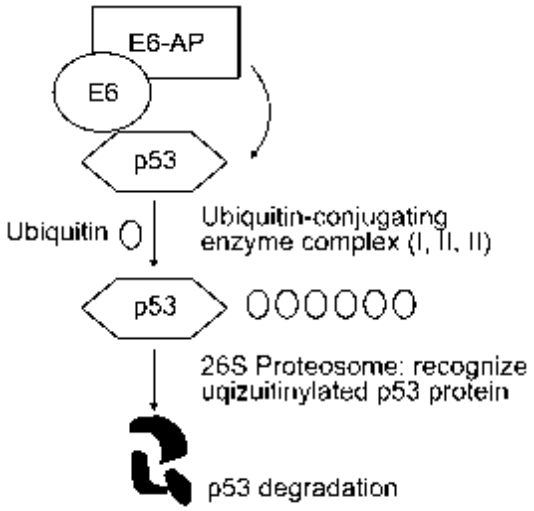

Figure 2 - Representation of the E6 protein-p53 tumor suppressor protein interaction. The E6 binds to E6-AP and to p53, which gets marked for ubiquitination mediated by the E6-AP and then suffers proteasomal degradation [16].

1.1.1.2 E7 oncoprotein

The E7 protein has approximately 100 amino acids and 25 kDa and its found mostly in the nucleus, but also in the soluble cytoplasmic fraction and nucleolus [22, 23]. There are three domains in the E7 protein called conserved regions (CR) – (CR1, 2 and 3) [24]. Two of these regions, the CR1 and CR2, share homology with SV40 T antigen and adenovirus E1A [25]. This homology is also conserved amongst different HPV E7 proteins and are separated by a non-conserved sequence of variable size and amino acid composition [22]. Both CR1 and CR2 are necessary for cellular transformation [26]. CR1 can stimulate the cellular transformation in a pRb-binding independent way, whereas CR2 associates with pRb through the conserved LXCXE (Leu-X-Cys-X-Glu) motif [25]. The HPV E7 protein is capable of associating with a group of proteins known as pocket protein family, such as the pRb and its related proteins p107 and p130, which act as negative regulators of cell growth, including in the G0/G1, G1/S and G2/M transitions [16, 18].

In a normal biological situation, when the pRb is hypophosphorylated, it binds to transcription factors of the E2F family. As these transcriptional factors are responsible for regulating the

expression of cellular genes that are involved in the DNA synthesis, like the DNA polymerase, by blocking its functions, the hypophosphorylated pRb negatively controls the progression of the cell cycle. As mentioned earlier, the E7 is able to form complexes with the pRb and its related proteins, preventing them to bind to the E2F that is now free to activate and stimulate the expression of several host genes necessary for DNA replication, allowing the cell to proliferate [11, 18]. It has been shown that the ability to disrupt the E2F-pRb complex is bigger for the high risk HPV E7 than it is for the low risk HPV E7 (figure 3) [25].

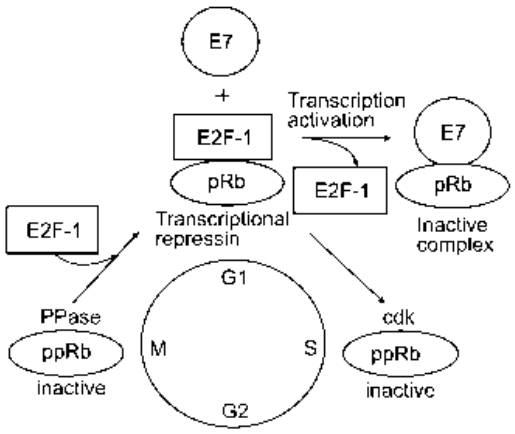

Figure 3 – Representation of the E7 protein-pRb protein. In physiologic conditions, the hypophosphorylated pRb form complexes with E2F, negatively regulating the progression of the cell cycle. When the infection occurs, the E7 binds to the hypophosphorylated pRb, which inhibits its binding to the E2F that stays free to stimulate transcription of DNA synthesis genes, allowing the cell cycle to progress [16].

1.1.2 Preventive Vaccines

It has been reported that HPVs are associated with approximately 99% of cervical cancers, particularly HPV type 16. Thus, HPV is a potential target for development of vaccines, being necessary a basic understanding of HPV biology [4]. There are two types of vaccines that can be used in cervical cancer or other HPV-associated malignancies. The first strategy is to prevent infection with preventive vaccines that are based on HPV virus-like particles containing HPV structural proteins and can generate neutralizing antibodies to block HPV infection. The second one is to eliminate HPV infection by inducing a virus-specific T cell-mediated response by the use of therapeutic vaccines [4, 10].

At present, there are two preventive vaccines (bivalent and quadrivalent) against HPV infection, also called prophylactic vaccines, both approved by the Food and Drug Administration (FDA) [3]. The quadrivalent one is called Gardasil®, developed by Merck (NJ, USA), and is expressed in yeast *Saccharomyces cerevisiae* [27]. Gardasil® acts successfully against infection by four of the most clinically relevant HPV types: the low risk HPV-6 and 11 and the high risk HPV-16 and 18 [10, 28]. The bivalent vaccine is called Cervarix®, developed

by GlaxoSmith-Kline (GlaxoSmith-Kline Biologicals, Rixensart, Belgium), and is expressed in an insect cell system [27]. This vaccine protects against HPV-16 and 18 and also does partial cross-protection against HPV-31 and 45, which are phylogenetically related to the two previous ones [28].

Both Gardasil® and Cervarix® contain a non-infectious recombinant L1 virus-like protein with the aim to generate neutralizing antibodies against major capsid protein, L1 [4]. They are highly immunogenic, have high avidity for the systemic antibody response and are capable of producing memory of B cell response, which enables the cell to make a rapid burst of antibodies upon a secondary exposure [10, 29]. Despite the L1 is not expressed in the basal cells infected with HPV, it still is deeply studied and targeted for preventive vaccines [4]. However, preventive vaccines are limited in their action to few types of HPVs, they do not have therapeutic effects against pre-existing HPV infections nor HPV-associated lesions and the vaccination program has relatively high cost [4, 30].

1.1.3 Therapeutic vaccines

As the name implies, preventive vaccines only have a preventive effect and can only be applied before the infection, unlike the therapeutic ones that can eliminate pre-existing lesions and even malignant tumors. To do that, it is important to select the ideal target antigen. As described above, HPV early proteins are expressed throughout the virus life cycle and help regulate progression of the disease. In particular, the HPV E6 and E7 proteins are of great interest for potential targets as they are essential to induce and maintain the cellular transformation and malignancy [31].

Nevertheless, before using E6 and E7 in DNA vaccines for human application and regarding safety, there is the need to eradicate their oncogenic potential. There are two ways to accomplish this: the first and most used one is to introduce point mutations that have been reported to prevent interaction of E6 with p53 and E7 with pRb. The second method is called ‘gene-shuffling’ and involves the rearrangement of the primary gene sequences, so the ligand binding domains are disrupted. To be sure that no loss of possible T-cell epitopes is caused, the original sequence junctions that are destroyed are added as an appendix [32].

1.2 DNA technology

In the last decades, the knowledge about genes and their function augmented significantly, allowing the discovery of recombinant DNA technology and gene cloning, in the 80s, and the increase in genomics data, in the 90s [33]. The decoding of the entire human genome has provided the knowledge to define some disease-causing genetic factors and the association between DNA (genes) and proteins have generated a fullness of potential therapeutic opportunities based on engineered genes and cells [33, 34].

Despite the evolution on the Biotechnology field, a great number of diseases are yet to be conquered, with millions of people dying each year due to the inefficiency of the current therapeutic methods [35]. To overcome the demands of present and emerging public health problems, some innovative therapeutic strategies are being developed, like gene therapy and DNA vaccines, that seem to be really promising [36].

1.2.1 Gene therapy

Gene therapy is the transfer of genetic material (DNA) to cells that have defective or mutant genes, creating a therapeutic effect, by either assisting or replacing the genetic defects or by overexpressing proteins that are therapeutically useful [33, 36]. By the definition of United States FDA, gene therapy is the product "that mediate their effects by transcription and/or translation of transferred genetic material and/or by integrating into the host genome and that are administered as nucleic acids, viruses, or genetically engineered microorganisms" [37]. Therefore, gene therapy uses genes as a medicine to cure, or at least to improve the clinical status of a patient, a broad spectrum of serious acquired and inherited diseases, namely cancer, acquired immunodeficiency syndrome (AIDS), cardiovascular diseases, infectious diseases and other [38, 39]. However, this is a complex process, since there is the need to ensure the arrival of the transgene into the nucleus without suffering any degradation. To overcome this obstacles, namely the degradation and the passing through the plasma membrane to the nucleus, it is necessary to use a gene delivery system [39]. This topic will be discussed later.

Gene therapy is generally classified into two categories according to the nature of the targeted cell: germ line gene therapy and somatic gene therapy. In the first one, the functional gene is inserted in the reproductive cells, like sperm or zygote, and thus it will be integrated into the individual genome and the modification might pass along to the next generation. In the second one, the transgene is inserted in the somatic cells (non-reproductive cells), narrowing the effects and modifications to the specific individual, not passing to the next generation. So far, the legislation only allows the use of somatic gene therapy, due to ethical reasons [37, 39]. The somatic gene therapy may also be divided into two different approaches: *ex vivo*, where the cells are removed from the patient's body, genetically manipulated and then returned to the patient's body, and *in vivo*, where the cells manipulation occurs in the patient's body. Both are under investigation and their great goal is to successfully deliver therapeutic genetic material to the target cells [40].

It is important to refer that up until now cancer composes over 60% of all ongoing clinical trials on gene therapy, followed by monogenetic and cardiovascular disease, being by far the most common disease treated by gene therapy [37].

1.2.2 DNA vaccines

Looking back to the past century, it can be said that the development and widespread use of vaccines against a large number of infectious agents have been a great triumph of medical science. It all started over 200 years ago when Jenner succeeded to show that prior exposure to cowpox could prevent infection by smallpox, emerging the concept of vaccination [41]. Despite this progress, as mentioned above, some diseases still cause death to millions of people. Hence, the world urgently requires new technologies able to respond quicker and that are able to be developed faster for new vaccines. An opportunity to answer this matter relies on DNA vaccines [42]. The DNA vaccination is a recent therapeutic strategy that is based on the use of a vector that encodes one or more antigens corresponding to the protein(s) of interest under a promoter, capable of function in the transferred cells [43].

Compared to the conventional vaccines, DNA vaccines have some advantages that are worth to considered, as briefly presented in table 2. A big difference between them is that the gene-based vaccines can generate both humoral and cellular immune responses [44].

Table 2 - Advantages of DNA vaccination (adapted from [45]).

Advantages of DNA vaccines comparing with conventional vaccines	
Design	DNA vector optimization through codon and ribonucleic acid (RNA) structure changes Can generate effective cytotoxic T lymphocyte and antibody responses Can be engineered to express tumor antigenic peptides or proteins Enables prolonged expression of antigens and enhancement of immunologic memory
Safety	Unable to revert into virulent forms, unlike live vector–based vaccines Capacity for repeated administration safely and effectively No significant adverse events in any clinical trial
Stability	Temperature-stable Long shelf life
Manufacture	Suitable for large scale production at high purity Rapid production and formulation Easy to store and transport

The DNA vaccination is capable of inducing the adaptive immunity, while producing antibodies and activating helper T cells and cytotoxic T cells, and even the innate immunity [46]. Upon DNA vaccine transfection, the host cell transcribes, translates and expresses the viral antigen [47]. When professional antigen presenting cells (APCs) encounter an exogenous

and foreign antigen, they take it up into their endolysosomal pathway. The protein is then processed and degraded to peptide fragments that are loaded and presented on the cell surface by the major histocompatibility complex (MHC) class II [35, 48]. This antigen peptide-MHC class II complex is recognized by specific helper T cells, the CD4+ T cells that can produce cytokines that will help in other cell activities. For example, they can help B cells generate effective antibody responses and/or help cytolytic T lymphocyte responses, depending on the cytokine [35, 41]. This via is known as humoral response (figure 4). Considering the antibody responses, B cells recognize and respond to extracellular antigens or exposed extracellularly antigens that belong to transmembrane proteins [35].

On the other hand, there is the cellular response, where the foreign protein can be intracytoplasmic and so it is processed by the proteosome into peptide fragments. The peptide fragments associate to MHC class I molecules, transported to the cell membrane and then are presented on the APC surface. This peptide-MHC class I complex is recognized by cytolytic T lymphocytes, the CD8+ T cells, that become activated also by the action of co-stimulatory molecules (figure 4) [35, 48].

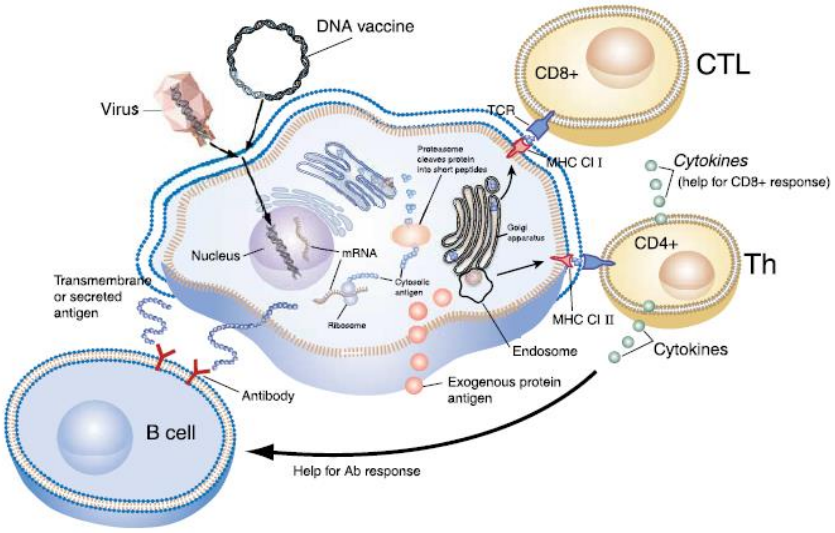

Figure 4 - Representation of the mechanisms of both humoral and cellular immune responses. DNA vaccination aims these two responses. If the foreign antigen is exogenous, it will be taken up by professional APCs into its endolysosomal pathway. The protein is degraded to peptide fragments, which are presented by the MHC-II and recognized by CD4+ T cells. These are activated to produce cytokines that help B cells to become activated and produce antibodies (humoral response) and also help cytolytic T cells response. The antigen can likewise be intracytoplasmic, being degraded by the proteosome into fragment peptides that are presented by the MHC-I to the CD8+ T cell, leading to its activation (cellular response) [35].

1.2.3 DNA delivery systems

The delivery of naked DNA to target cells for therapeutic purposes has its drawbacks, as it is susceptible of degradation by endonucleases, its crossing through the cell membranes is

limited by its net negative surface charge and large hydrodynamic diameter and if it is endocytosed it may be degraded by the endolysosome. To ensure that none of these occurs, it is imperative to use a DNA delivery system [49]. The ideal DNA delivery system, also known as vector, must not trigger a strong immune response, it must be capable of transporting the DNA independently of its size and deliver the transgene to target cells, it must be episomal or integrate into a specific genome region without randomly integration and it must be easily prepared, not expensive and available at high concentrations commercially [39]. Currently, there are two types of available vehicles for gene delivery: the viral and nonviral vectors [50].

1.2.3.1 Viral vectors

Viruses have a number of biological properties that made them one of the first choices for gene delivery vehicles: they can recognize and enter cells, specifically penetrate into the host cell nucleus and then take advantage of the cellular machinery and express its own genetic material and replicate it in the host cell and spread to other cells [39, 51]. Before using a virus as a gene transfer vector, it must be modified by genetic engineering, in order to reduce patho/immunogenicity. To accomplish this, the dispensable and pathogenic genes are removed and replaced by the gene(s) of interest. On the other hand, the viral genes that are necessary for the assembly of viral particles, the packing of the viral genome into particles and the therapeutic gene delivered to the target cells still remain in the vector construction [39, 50]. The main viruses used on gene delivery are adenovirus, adeno-associated virus, lentivirus, retrovirus and also herpes simplex virus. These viral vectors are the most used system to transfer genes, because they have high transfection efficiency, but they also have some downsides, as briefly presented in table 3 [39].

Table 3 - Advantages and disadvantages of the main viral vectors [34].

Viral vector	Advantages	Disadvantages
Adenovirus	High transfection efficiency	Strong immune response
	Transfects proliferating and non-proliferating cells	Insert size limit of 7.5 kbp
	Substantial clinical experience	Difficult to manufacture and quality control
		Poor storage characteristics
		Short duration of expression
Retrovirus	High transfection efficiency	Low transfection efficiency *in-vivo*
	Fairly prolonged expression	Insert size limit of 8 kbp *ex-vivo*
	Low immunogenicity	Transfects only proliferating cells
	Substantial clinical experience	Difficult manufacture and quality control
		Safety concerns (mutagenesis)
Lentivirus	Transfects proliferating and non-cells	Very difficult manufacture and quality control
	Transfects haematopoietic stem cells	Poor storage characteristics
		Insert size limit of 8 kbp
		No clinical experience
		Safety concerns (origins in HIV)
Adeno-associated virus	Efficient transfection of wide variety of cell types *in-vivo*	Difficult manufacture and quality control
	Prolonged expression	Insert size limit of 4.5 kbp
	Low immunogenicity	Safety concerns (mutagenesis)
		Limited clinical experience

1.2.3.2 Nonviral vectors

As presented in table 3, the viral vectors have disadvantages that have to be seriously considered, like the capacity to cause several immune responses. This has led to the need of finding safer alternatives and nonviral vector delivery systems are emerging as a favorable solution to overcome some of the viral vector drawbacks [52]. Comparing to viral vectors, the nonviral vectors are relatively safe, have low immunogenicity and less toxicity, have easy formulation and assembly and can be prepared in large quantities at low cost. Furthermore, they are capable of transferring different and larger therapeutic genes, with no limit on size,

and because of their stability they can be stored for long periods [34, 39]. Unfortunately, their use in large amounts is limited by their low transfection efficiency [39].

There are two categories when considering nonviral DNA delivery systems: the physical and the chemical one. The physical approach is applied when the DNA delivery into the target cells is made by the use of physical forces that weakens the cell membrane, causing it to be temporarily permeable, which facilitates the diffusion of the transgene. This process is not mediated by a carrier. The physical methods include needle injection, electroporation, gene gun, ultrasound and hydrodynamic injection. The chemical approach occurs when the DNA is delivered into the target cell nucleus by a carrier that can be prepared by several types of chemical reactions [39, 53]. Within this group, the most studied strategy so far has been the formulation of DNA into condensed particles by using cationic lipids or cationic polymers. Hence, these particles suffer cell endocytosis, macropinocytosis or phagocytosis as intracellular vehicles, from which a small part of the DNA is released into the cytoplasm and migrates into the nucleus, where the therapeutic gene is expressed [53]. Our research group has been conducting several studies with nanoparticles, including chitosan nanoparticles for the delivery of p53 sc pDNA [54]. The subject-matter of nanoparticles will be discussed later.

1.3 Plasmid DNA

Within the huge variety of vectors for gene delivery, there is the pDNA. Because of its safety, its easiness of production on a large-scale, its simple application and also the fact that it does not cause toxicity, the pDNA has received an increased attention and has gained a huge interest for therapeutic applications [49]. It is used to deliver the desired genetic information into the target cells and to induce the production of the relevant proteins. Consequently, in the past few years, the use of pDNA as a delivery system on approved gene-therapy protocols has increased exponentially, representing 64.4% of the gene therapy clinical trials in 2016 [55].

Plasmids are double-stranded DNA molecules that are covalently closed. Each strand is a linear polymer of deoxyribonucleotides that are linked by phosphodiester bonds, negatively charged at pH>4 [42]. The two strands wind in an anti-parallel sense around each other and around a common axis that forms the double helix structure, stabilized by hydrogen bonds and stacking forces [56]. This structure has a hydrophilic backbone, composed by sugars and phosphate groups, and a hydrophobic interior, composed by planar aromatic bases stacked on each other. pDNA can have different sizes and normally they are small (2 to 20 kbp and a molecular weight of 106 to 107 Daltons), although they are very large when compared with proteins [56, 57]. Despite this, in the future it will be needed multigene vectors, including extensive control regions, that may require the production of larger plasmids [58]. The pDNA molecule can be coiled in space, causing the formation of a higher order molecule known as sc pDNA [56]. The active sc pDNA form, also called covalently closed circular DNA (cccDNA), is

the main one, but under stress or unfavorable environment conditions, such as extreme pH or high temperature, it can generate other forms [57]. The other topological pDNA conformations can be the open circular (oc) or the linear form, caused by single-stranded and double-stranded nicks, respectively [42]. Linear and oc pDNA isoforms are formed by random nick(s) that might damage at different gene locations, such as the promoter or gene coding regions that become destroyed, and so they are inefficient to induce the expression of the therapeutic gene [57]. Therefore, the sc pDNA is the most appropriate and desired form for therapeutic applications [59].

By estimates, it is known that only one per thousand plasmid molecules presented to the cells reaches the nucleus and is expressed [60]. Thus, there is the need to improve the current strategies of sc pDNA production, so it may be of high copy number, highly pure and successfully delivered to the targets cells. Moreover, it is also important to develop adequate delivery systems that protect pDNA vector from degradation and also that facilitates the entrance and delivery to the nucleus of the higher number of pDNA.

1.3.1 pDNA manufacture

The manufacture of pDNA is divided into three different stages: upstream processing, fermentation and downstream processing (figure 5). Firstly, there is the construction and selection of an appropriate plasmid vector and production of microorganisms, followed by selection and optimization of the fermentation conditions and cell growth and then the isolation and purification steps, with the aim of producing large quantities of stable and highly purified sc pDNA [61].

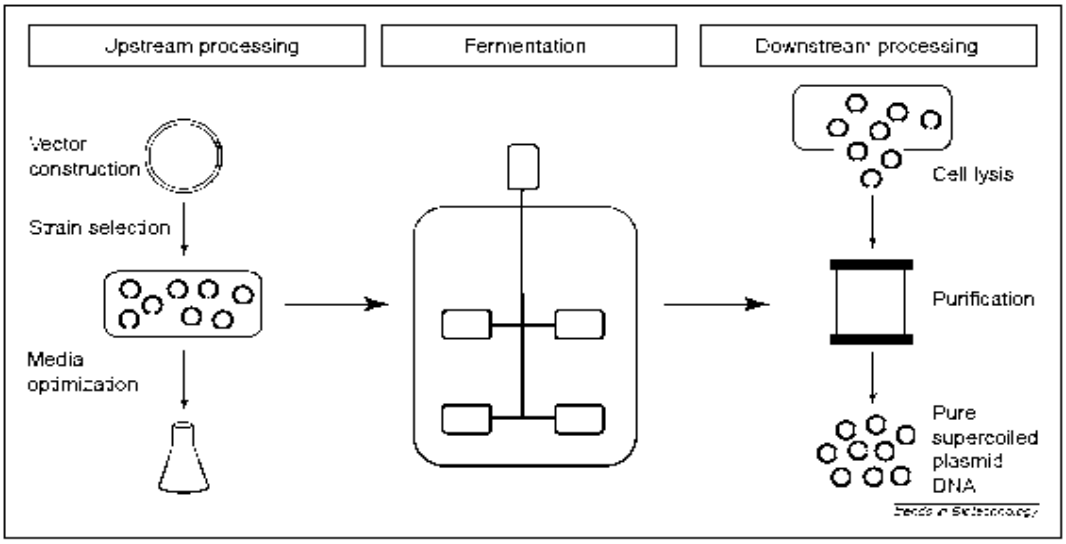

Figure 5 - Representation of the three essential stages to obtain pure sc pDNA [61].

When the purpose is pDNA vaccination, the design of the pDNA vector must include some typical elements, such as an origin of replication for efficient propagation in the adequate

host cell, a selectable marker like an antibiotic resistance gene for growth selection, a strong eukaryotic promoter to drive expression, a polyadenylation signal to terminate the transcription and the transgene that encodes the antigen of interest (figure 6) [62].

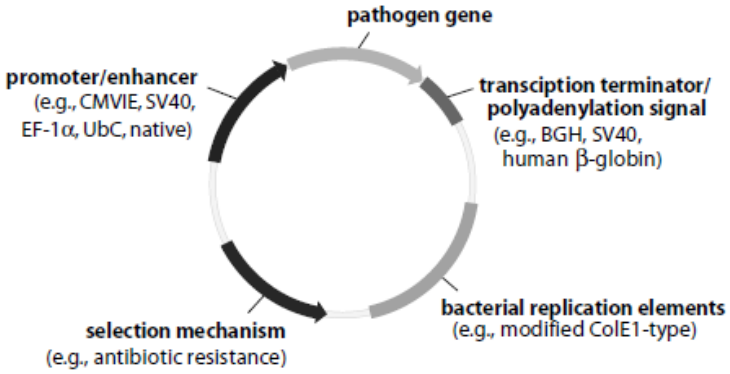

Figure 6 - Representation of the construction of the plasmid DNA [62].

The typical host used in fermentation is *E. coli*. To obtain the pDNA, the cells are usually disrupted by alkaline lysis [56]. Unfortunately, the pDNA only represents around 3% mass/mass (w/w) of the *E. coli* extract [63]. To eliminate some of the impurities, it follows a primary isolation process that involves clarification and concentration steps [57]. This allows the removal of some impurities like RNA, genomic DNA (gDNA), endotoxins and proteins [63]. Lastly, a chromatographic purification step is used to separate sc pDNA from structurally related impurities, like relaxed and denatured pDNA, gDNA, low molecular weight RNA and endotoxins [61].

1.3.2 pDNA purification

With the progress in therapeutic approaches, emerges the need to develop a good pDNA purification process, in order to obtain sc pDNA homogeneity near to 100% and to follow the quality specifications recommended by the regulatory agencies, such as FDA and the European Medicines Evaluation Agency (EMEA) [56, 64]. At present, liquid chromatography is the central technology used in pDNA purification, as it is simple, robust, versatile and it has high resolution and high reproducibility [57, 65]. Despite its plusses, chromatography has a challenge when it comes to the separation of pDNA from the contaminants, because they share similar characteristics, like the negative charge (RNA, gDNA, endotoxins), similarity in size (gDNA, endotoxins) and hydrophobicity (endotoxins) [63]. Numerous chromatography processes have been developed by exploring different properties including charge, molecular size, hydrophobicity and affinity [56].

1.3.2.1 Size exclusion chromatography

Size exclusion chromatography can fractionate and purify plasmids from a clarified lysate based on the wide variety of molecular mass. The larger molecules, like pDNA and gDNA, are

incapable of penetrate the pores, eluting first, so they can be separated from the smaller ones, like RNA, endotoxins and proteins [42, 57]. But because the lysate is a complex mixture of different molecules, the resolution here is limited, as well as the isolation of sc pDNA in one single step [57].

1.3.2.2 Anion exchange chromatography

Anion exchange chromatography is based on the interaction between the negatively charge phosphate groups in the DNA backbone and the positively charged ligands on the stationary phase [56]. After the binding occurs, it is applied an increasing salt concentration to displace and elute the different nucleic acids by order of an increasing overall net charge, which is function of chain length and conformation [65]. Given that sc pDNA is more compact and has higher charge than the oc pDNA, it is possible to separate these two isoforms [42]. Nevertheless, this type of chromatography presents poor selectivity towards pDNA and impurities, like RNA, gDNA and endotoxins, due to their similar binding affinities, making the purification of pDNA insufficient [66].

1.3.2.3 Hydrophobic interaction chromatography

Hydrophobic interaction chromatography relies on the differences in the hydrophobic interactions of pDNA, single-stranded nucleic acid and endotoxins, using high salt concentration for the biomolecules retention [57]. To elute the bound species, the salt concentration of the mobile phase is decreased, weakening the hydrophobic interactions and the elution occurs by increasing the hydrophobicity order. This property is mainly defined by base composition, size and structure [56, 57]. This technique is inefficient on separating different pDNA isoforms and in addition the use of high salt concentration, which is associated with higher costs and environmental impact, is also a downside [57, 67].

1.3.2.4 Affinity chromatography

Affinity chromatography (AC) is a separation technique that exploits natural biological processes like molecular recognition for the selective purification of target biomolecules based on their biological function or chemical structure [42]. The high specificity and efficiency of affinity interactions allow this method to eliminate additional steps, to increase yields and to improve process economics [57, 66]. Nonetheless, it has some limitations, as the fragility and low binding capacity of the biological ligands. To overcome this, synthetic ligands were designed, combining the selectivity of natural ligands with the high capacity and durability of synthetic systems [57].

This purification method separates biomolecules based on reversible interactions between the target one and its specific ligand that is immobilized on the chromatographic matrix [57]. Under appropriate pH and ionic strength, the sample is injected onto the column and the target biomolecule binds to the specific ligand [68]. After, elution steps are performed, being

specific with a competitive ligand or non-specific with a change in pH, ionic strength or polarity, depending on the matrix and the characteristics of the biomolecule [57].

The interactions between target biomolecule and its ligand result of the combination of electrostatic interactions, hydrophobic interactions, van der Waals forces and/or hydrogen bonding. As these interactions are so specific, they represent a crucial advantage of AC, because they allow to obtain high selectivity and high resolution [57].

Within AC, there are several types like immobilized metal-ion, triple-helix, polymyxin B, protein-DNA and amino acid-DNA [57]. For the purpose of this project, we will only focus on the last method.

1.3.2.4.1 Amino acid-DNA AC

The use of amino acids in AC has already demonstrated to be efficient on the successful biorecognition of the sc isoform, by using a single purification step.

Amino acids have been of great use in biotechnology applications, since they are natural compounds that can be safely used in pharmaceutical applications [42, 69]. Besides, based on atomic studies, amino acids preferentially promote specific interactions with nucleic acid bases, especially the positively charged ones like histidine, lysine and arginine [69]. The use of these amino acids as ligands has allowed an efficient purification of sc pDNA and the recognition of this isoform proved the presence of specific interactions between pDNA molecule and the amino acid-based matrices [70].

In fact, our research group has already showed the successful application of some amino acids for the purification of pDNA. For instance, the use of lysine and histidine for the separation of sc pDNA from a clarified lysate sample resulted on a high purity degree of this biomolecule of interest, being in accordance with the regulatory agencies specifications [64, 66, 71]. Nonetheless, the overall recovery yield of these two strategies was low: 45% and 40%, respectively [66, 71]. On the contrary, the use of arginine on the affinity chromatography resulted on a recovery of 79% of sc pDNA and also a high purity degree, under mild elution conditions, thus representing a smaller environmental impact [72].

Taking this into account, the arginine amino acid reveals itself to be a good affinity ligand to purify the sc pDNA, due to its high selectivity for the sc pDNA recognition and thus high recovery and purity. Despite this, the conventional stationary phases have some drawbacks, like the low capacity, working at low flow rates that results in longer retention time and possible degradation of the target biomolecule [73]. Consequently, raises the need to explore alternative chromatographic supports.

1.3.3 Monoliths: innovation on chromatographic supports

As discussed above, the studies with affinity matrices have revealed positive results, however there are still some limitations to be surpassed. Monoliths have been gaining attention owing to their appealing properties. Considered the fourth generation of the chromatographic stationary phases, a monolith is a continuous and highly porous bed; the pore size is adjustable considering the desired application, depending on polymerization process [68, 70, 74]. They are polymerized into a column as a single unit and thus the scale-up and scale-down variations in packing quality and the need to repack the column because of the appearance of air bubbles are eliminated [74]. Monoliths exhibit increased permeability and interconnectivity, allowing high mass transfer and more access to binding sites for the target biomolecule, having a very high binding capacity for pDNA [68]. Additionally, this innovative support has flow independent resolution, allowing the same separation and resolution even working at high flow rates. This enables a very fast separation and reduced retention time, which ensures less biomolecule degradation [70, 73, 74].

Bearing all this positive characteristics in mind along with the amino acids', combining a monolithic support with amino acids ligands or derivatives for the purification of sc pDNA using AC has been a promising and favorable strategy.

For instance, our research group has already demonstrated that arginine monolith allows the separation of a sc pDNA, at a laboratorial scale, with 86% of purity. This support was also characterized in terms of dynamic binding capacity (DBC), which has presented a higher value that the equivalent conventional support [75]. On the other hand, agmatine and histamine monoliths also revealed themselves to be efficient at separating sc pDNA, with 99.6% and 96.66% of purity, respectively [76, 77]. Thus, the monolithic approach allows higher selectivity for the sc pDNA and higher binding capacity.

1.4 Nanotechnology

Nanotechnology is a recent and promising field that involves multiple disciplines and within it there is the Cancer Nanotechnology, which includes the use of nanoparticles to detect and treat cancerous cells [78, 79]. As previously mentioned, estimates indicate that only one per thousand plasmid molecules presented to the cells reaches the nucleus and is expressed [60]. Thus, there is the need to create and develop strategies that help protect vectors, like pDNA, from degradation and that facilitates the entrance into the nucleus. Nanoparticles emerge as a good solution, offering many advantages over the delivery of free pDNA: they protect the therapeutic cargo against enzymatic degradation; they allow more specific targeting and delivery; by targeting to specific cells, there is an improvement of distribution and reduction of side-effects; the therapeutic cargo is more probably delivered to the desired intracellular compartment, with an improvement of cellular penetration [80–82].

1.4.1 Cellular trafficking of pDNA – barriers to cross

The pDNA vector comes across several physical barriers before it can finally enter the nucleus, where it should be expressed into the protein(s) of interest (figure 7). The first one is the plasma membrane, since it is negatively charged, like the pDNA, due to the glycosaminoglycan groups [80, 83, 84]. This causes electrostatic repulsions between the cell surface and the pDNA, preventing the last to readily crossing the plasma membrane, thus lowering the number that can actually enter the cell. If pDNA is delivered by nanoparticles, its entrance into the cell is higher. In general, nanoparticles are immobilized on the cell surface, due to non-specific electrostatic interactions or receptor-mediated ligand interactions, and then suffer internalization via endocytosis [80, 84]. The uptake of nanoparticles can be facilitated and enhanced by 'active targeting', which is accomplished by coupling ligands to them that must target them to specific cells, ensuring an efficient internalization by endocytosis [80]. Endocytosis results in the formation of endosomal vesicles, which represent another barrier for an efficient transfection [84, 85]. These vesicles – endosomes – have an internal pH around 5 and mature from early to late endosomes, before fusing with lysosomes that contain digestive enzymes. Hence, it is crucial that the nanoparticles with the nucleic acid cargo escape the endosome promptly, avoiding the enzymatic degradation within the lysosomes [86]. A way to escape the endosome is increasing endosomal osmotic pressure [87]. Depending on several factors, like composition, some nanoparticles are dissolved in the low acidic medium of endosomes. An example of these nanoparticles is the inorganic ones, which will be presented later. This dissolution destabilize the endosome through osmotic imbalance, disrupting the endosome membrane, enabling the cargo delivery into the cytosol [88]. Now, the pDNA must reach the nucleus for expression. The nuclear membrane represents another barrier. The crossing of this membrane could be through the nuclear pores, but they are size-limited and generally too small for free diffusion of plasmids [80, 84]. Despite this, plasmids are capable of reaching the nucleus during mitosis, due to an increase in the nuclear permeability [89].

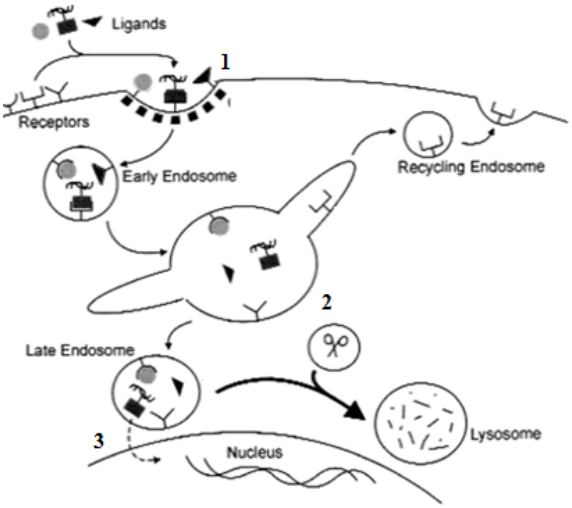

Figure 7 - Representation of the cellular trafficking of pDNA within the nanoparticles and the barriers that it has to overcome: 1 – crossing the plasma membrane; 2 – avoiding lysosomal degradation; 3 – crossing nuclear membrane [90].

1.4.2 Nanoparticles

As mentioned before, nanoparticles have the main goal of protecting and helping the delivery of the therapeutic molecules, like the pDNA vector. Besides, the ideal nano-carrier presents good biodistribution, has no toxicity with reduced side-effects and inflammation and allows the therapeutic cargo to be delivered to a specific target cell [80]. These carriers can have several types of composition, like phospholipids, lipids, dextran, chitosan, polymers, carbon, silica, metal and many other [81]. Taking into account the manufacturing method and the material used, the nanoparticles can be of various shapes and sizes, along with diferent characteristics (figure 8) [91].

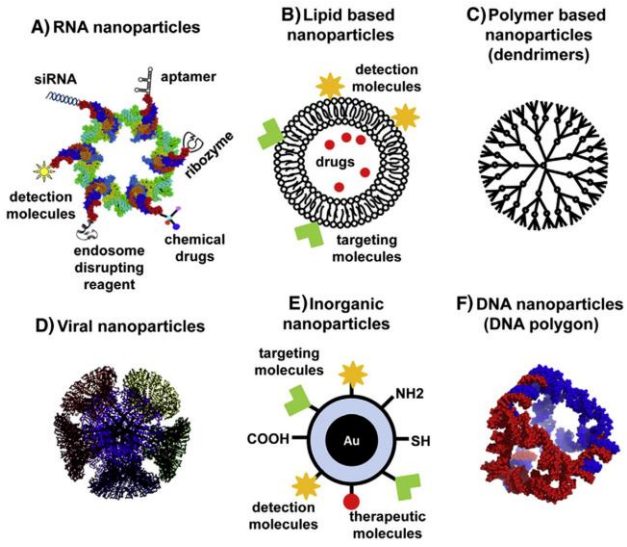

Figure 8 – Several examples of nanoparticles with diferent materials, sizes and structures [92].

The world of nanoparticles is tremendous and has developed a lot, however there is still much to improve and many limitations to overcome. For instance, some delivery systems still present cytotoxicity and low amount of gene expression in the target cells [93]. The use of inorganic nanoparticles might eliminate limitations of other nano-carriers, because they have good biocompatibility and low toxicity, mild preparation conditions, they are relatively inexpensive, they possess the ability for loading different therapeutic agents and a pH dependent dissolution that favors intracellular delivery [93–95]. Moreover, they are not subjected to microbial attack and exhibit excellent storage ability, facts that cannot be pointed out to the organic ones [93].

1.4.2.1 Mg_2CO_3 Nanoparticles

Nano-carriers based on calcium carbonate ($CaCO_3$) have already been described as a good delivery system [94, 96, 97]. Our research group has also obtained satisfactory results with this system [95]. pDNA/$CaCO_3$ nanoparticles are produced by co-precipitation of Ca^{2+}, an inorganic cation, with DNA, in the presence of CO_3^{2-}, an inorganic anion. Taking into account that these nanoparticles are already well-described and present good results, a small alteration can be performed to this delivery system - the Ca^{2+} substitution by other divalent ion, magnesium (Mg^{2+}), to investigate if the pDNA/$MgCO_3$ nanoparticles present even better results at gene transfection. Although the co-precipitation technique is simple and rapid, it can create precipitates, resulting in large nanoparticles, which in turn has negative effects on the cellular uptake and gene transfection. Thus, to increase the stability and the transfection efficiency of the proposed nano-carrier, a cationic polymer, gelatin, can be added to the nanoparticles. The use of gelatin, a biocompatible and biodegradable polymer, leads to the formulation of nanoparticles with enhanced properties concerning size, surface charges and gene delivery efficiency [98].

Chapter II - Global aims

The main objective of the present work is to obtain a pure DNA vaccine to prevent or treat the cervical cancer caused by HPV infection and create an appropriate delivery system that can protect and specifically deliver the DNA vaccine. In order to achieve this purpose, the sc pDNA must be highly pure, considering safety concerns recommended by the regulatory agencies. Hence, after the production of the pDNA in the recombinant *E. coli* host, the purification strategy has to be explored and optimized, maximizing the sc HPV-16 E6/E7^{MUT} pDNA recovery and purity degree. After the purification step, nano-carriers will be formulated with the purpose of protection, targeted delivery and enhancement of transfection. Then, the nano-carriers will be characterized to assure that they have the best properties and conditions to enhance the gene transfection and the therapeutic effects. At last, the transfection efficiency will be evaluated.

Overall, the goals are the optimization of the sc HPV E6/E7^{MUT} pDNA purification by the arginine monolith with spacer arm, the formulation of adequate nano-carriers for gene transfection and evaluation of the gene transfection efficiency.

Chapter III – Materials and methods

3.1 Materials

The chromatographic experiments were performed using the *AKTA Püre* system (GE Healthcare Biosciences Uppsala, Sweden), with a separation unit and a computer with Unicorn 6.3 software. Four epoxy monoliths (non-modified, modified with the 2-allyloxyethanol spacer arm, modified with arginine amino acid and modified with the 2-allyloxyethanol spacer arm and arginine) of 0.34 mL column bed volume were kindly prepared and provided by BIA Separations (Ajdovščina, Slovenia). For the pDNA pre-purification, it was used the *Qiagen Plasmid Purification Maxi Kit* from *Qiagen* (Hilden, Germany). Ethylene-diamine tetraacetic acid (EDTA), NaCl and ammonium sulfate ($(NH_4)_2SO_4$) were acquired from *Panreac* (Barcelona, Spain) and tris (hydroxymethyl) aminomethane (Tris) from *Merck* (Darmstadt, Germany). All of the solutions necessary for the chromatographic experiments were prepared with deionized ultra-pure grade water, purified with *Milli-Q* system from *Millipore* (Billerica, MA, USA) and analytical grade reagents. The elution buffers were previously filtered through a membrane with pores of 0.20 µm (Schleicher Schuell, Dassel, Germany) and sonicated ultrasonically. For the gDNA quantification, it was used the *iQ SYBR Green Supermix* (Bio-Rad, Hercules, CA, EUA).

3.1.1 Plasmid DNA

The 8.702 kbp HPV-16 E6/E7 plasmid vector was purchased from Addgene (plasmid 8641) (Cambrige, MA, USA) [99]. This vector contains the human beta-actin mammalian expression promotor and the ampicillin resistance gene (figure 9).

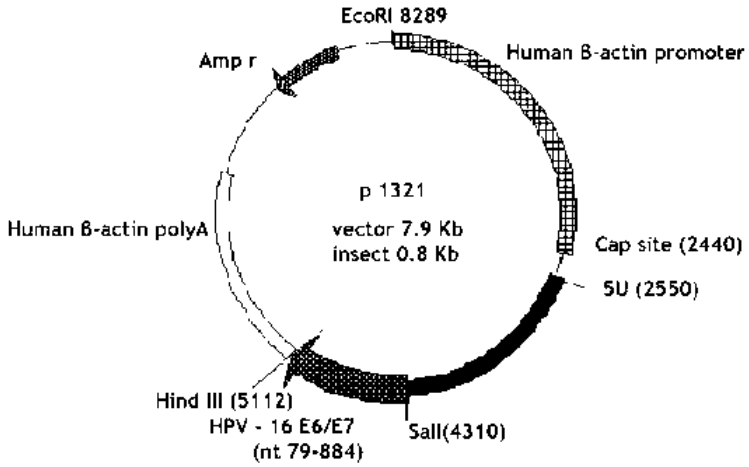

Figure 9 - Representation of HPV-16 E6/E7 pDNA.

E6 and E7 genes were mutated in different points to prevent the oncogenic role of the respective proteins, thus avoiding the recognition by the p53 and pRb tumor suppressor

proteins. The HPV-16 E6/E7 mutated (HPV-16 E6/E7^{MUT}) was prepared by NZYtech (NZYtech, Lisbon, Portugal).

3.2 Methods

3.2.1 Bacterial growth conditions

The HPV-16 E6/E7^{MUT} plasmid amplification was obtained by *E. coli DH5a* fermentation. The cells were plated on LB-agar medium with ampicillin and they grow overnight at 37 ºC. The colonies were then inoculated in Terrific Broth medium (20 g/L tryptone, 24 g/L yeast extract, 4 mL/L glycerol, 0.017 M KH_2PO_4, 0.072 M K_2HPO_4), complemented with 100 µg of ampicillin/mL and the growth was run at 37 ºC, under 250 rpm shaking. The bacterial growth was interrupted at the OD_{600}≈7 and the cells were recovered by centrifugation, at 3900 g for 10 minutes (min) at 4 ºC and the pellets were stored at 20 ºC.

3.2.2 Alkaline lysis with *Qiagen* Kit

The pDNA was obtained by alkaline lysis, with the *Qiagen Plasmid Purification Maxi Kit*, following the protocol provided by the manufacturer. Then, the binding of pDNA to the *Qiagen* Anion-Exchange columns was promoted under appropriate low salt concentrations and pH conditions. After the binding of the pDNA to the columns, a wash was made under a medium salt concentration, eluting the impurities (RNA, proteins and others impurities of low molecular weight). To elute the pDNA, a buffer with high salt concentration was used. Lastly, the pDNA was concentrated by isopropanol precipitation. The final pre-purified sample was used in some chromatographic experiments and DBC studies.

3.2.3 Modified alkaline lysis

The cells obtained from fermentation were lysed by a modified alkaline lysis method [100], as previously described [101]. The pellet was ressuspended in 20 mL of solution I (50 mM glucose, 25 mM Tris-HCl and 10 mM EDTA, pH 8.0). To perform the alkaline lysis, it was added 20 mL of solution II (200 mM NaOH and 1% (w/v) sodium dodecylsulfate (SDS)) and incubation at room temperature during 5 min. To neutralize the previous solution, it was added 20 mL of solution III (3 M potassium acetate, pH 5.0), followed by 20 min of incubation in ice. There were made two centrifugations (30 min and 20 min), at 20 000 g and 4 ºC, with an *Allegra*$_{TM}$ 25R centrifuge (Beckman Coulter, Miami, FL, USA), so the cellular debris, some gDNA and proteins were eliminated. Then, to precipitate the pDNA, it was added 0.7 volumes of isopropanol and incubated in ice (30 min). The precipitate was recovered by centrifugation (16000 g, 30 min, 4 ºC). The resulting pellet was dissolved with 1 mL of 10 mM Tris and 10 mM EDTA (Tris-EDTA), pH 8.0. To precipitate protein and RNA, it was added ammonium sulfate up to a final concentration of 2.5 M and incubation in ice during 15 min. Next, impurities were removed by centrifugation, 16000 g, 20 min, 4 ºC. To remove the salt, the sample was passed through the PD-10 column, using Tris-EDTA, pH 8.0 elution buffer, according to the

manufacturer's instructions. EDTA was added to the elution buffers to stabilize the pDNA, avoiding its degradation.

3.2.4 Affinity Chromatography

All chromatographic experiments were performed using an AKTA Pure system. In order to characterize the chromatographic behavior of each monolith (non-modified, modified with the 2-allyloxyethanol spacer arm, modified with arginine amino acid and modified with the 2-allyloxyethanol spacer arm and arginine) with a pre-purified pDNA sample, linear gradients were performed by decreasing the ammonium sulfate concentration from 3 to 0 M or increasing the NaCl concentration from 0 to 3 M.

Several elution strategies were explored in the arginine monolith with spacer arm with a lysate sample, by increasing the NaCl concentration, pH manipulation from 6.5 to 9 and addition of arginine in the elution buffer as a competition agent, to determine the optimal conditions for the sc pDNA isolation. Thus, the sc pDNA purification was achieved at laboratorial scale, by injection of 200 µL of lysate sample and by increasing stepwise gradient from 680 mM NaCl in Tris-EDTA, pH 7 to 649 mM and 1 M NaCl in Tris-EDTA, pH 7.5, at 1 mL/min.

To evaluate the applicability of arginine monolith with spacer arm in the sc pDNA purification at preparative scale, the column was equilibrated with the conditions described above and overloaded with 68 mL of lysate sample (5 µg of pDNA/mL), prepared in the same equilibrium buffer. After that, it was used the same elution strategy described above. All the experiments were carried out at room temperature and the absorbance was constantly monitored at 260 nm. Fractions were collected according to the obtained chromatograms, concentrated and desalted with Vivaspin® 6 Centrifugal Concentrator (Vivaproducts, Littleton, MA, USA) at 1000 g for further electrophoretic analysis and impurity (gDNA, proteins and endotoxins) quantification.

3.2.5 Agarose gel electrophoresis

The pooled fractions from each chromatographic experiment were analyzed by horizontal electrophoresis in a 15 cm long of 0.8% agarose gel (Hoefer, Holliston, MA, USA) and stained with Greensafe (0.012 µL/mL) (NZYTech, Lda. – Genes and Enzymes, Lisbon, Portugal). Electrophoresis was made at 120 V, during 30 min, with TAE buffer (40 mM Tris base, 20 mM acetic acid and 1 mM EDTA, pH 8.0). The gel was then visualized under ultraviolet (UV) light in a FireReader (Uvitec Cambridge, UK).

3.2.6 Supercoiled plasmid DNA quantification

The pDNA purity and recovery yield from the recovered fractions of the chromatographic experiments were evaluated with the CIMac™ pDNA analytical column, by applying a modified

analytic method, as previously described [77] and using an AKTA purifier system (GE Healthcare Biosciences, Upssala, Sweden) with a Unicorn 5.11 software. A calibration curve was constructed using pDNA standards from 1 to 50 µg/mL (figure 10). The pDNA standards were obtained by dilution of the highest concentration of sc pDNA with 200 mM Tris-HCl, pH 8.0, and the respective concentrations were confirmed by Ultrospec 3000 UV/Visible Spectrophotometer (Pharmacia Biotech, Cambridge, England). Firstly, the column was equilibrated with 600 mM NaCl in 200 mM Tris-HCl, pH 8.0 and 20 µL of sample was injected, at 1 mL/min. After, a linear gradient from 600 mM to 700 mM NaCl in 200 mM Tris-HCl (pH 8.0) was applied for 10 min, eluting all pDNA isoforms. Purity degree was calculated through the ratio between sc pDNA peak area and total peak area in the analytical chromatogram and the recovery yield through the ration between the recovered sc pDNA concentration and the sc pDNA concentration from the lysate sample.

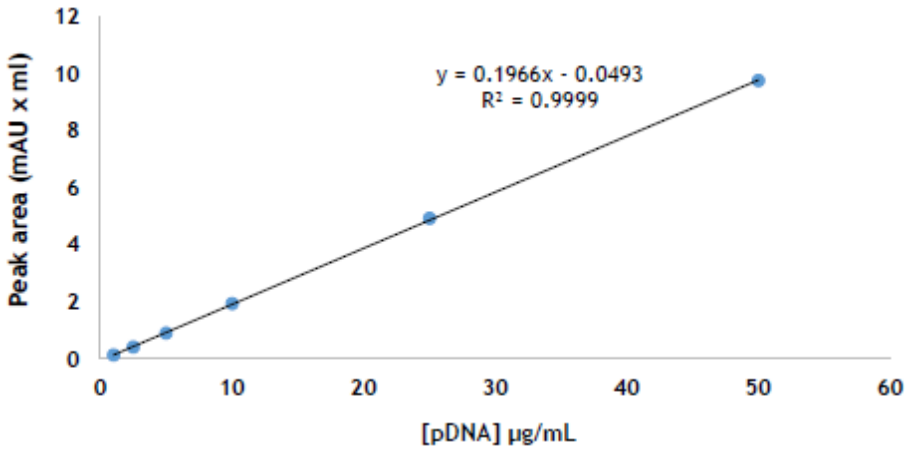

Figure 10- Calibration curve with pDNA standards (1 - 50 µg/mL).

3.2.7 Protein quantification

The protein concentration was measured by the micro-bicinchoninic acid (BCA) protein assay from Pierce (Rockford, USA). The quantification consists on adding 50 µL of each sample to 200 µL of BCA reagent in a microplate and 30 min of incubation at 60 ºC. Then, absorvance was measured at 595 nm in microplate reader (Biochrom, Cambridge, United Kingdom). The calibration curve was constructed with Bovine Serum Albumin (BSA) (St. Louis, MO, United States of America) as a standard protein (20-2000 µg/mL) (figure 11).

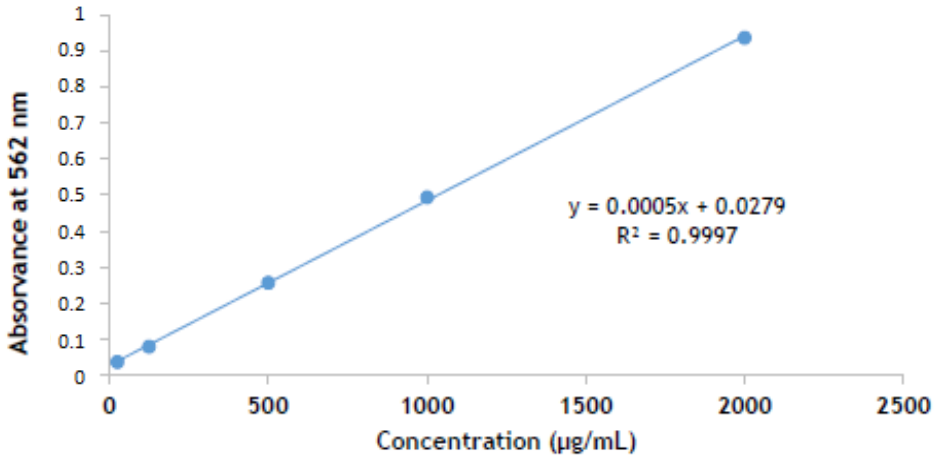

Figure 11 - Calibration curve with Bovine Serum Albumin standards (20 – 2000 µg/mL).

3.2.8 Genomic DNA quantification

The quantification of gDNA was obtained by real-time polymerase chain reaction (PCR) in a iQS Multicolor Real-Time PCR Detection System (BioRad), according to instructions described by Martins *et al*. [102]. Sense (5'-ACACGGTCCAGAACTCCTACG-3') and antisense (5'-CCGGTGCTTCTTCTGCGGGTAACGTCA-3') primers were used to amplify a 181-bp fragment of the 16S rRNA gene. PCR amplicons were quantified by following changes in fluorescence of the DNA binding dye Syber Green I. The calibration curve was constructed by a serial of dilutions of the *E. coli DH5a* gDNA sample, purified with the Wizard gDNA purification kit (Promega) in the range of 0.005 to 50 ng/mL (figure 12).

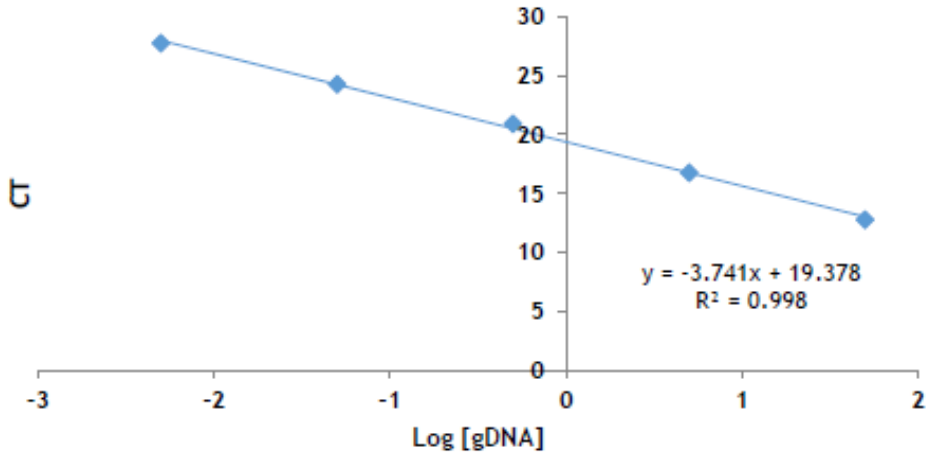

Figure 12 - Calibration curve of *E. coli DH5a* genomic DNA standards (0.005 – 50 ng/mL).

3.2.9 Endotoxin quantification

Endotoxin content was measured by ToxinSensorTM Chromogenic Limulus Amoebocyte Lysate (LAL) Endotoxin Assay Kit from GenScrip (USA, Inc.), following the manufacturer's instructions. The calibration curve was constructed with 10 EU/mL stock solution provided with the kit (0.01-0.1 EU/mL) (figure 13). Samples to analyze and samples from the kit were

diluted and dissolved, respectively, with non-pyrogenic water, which was also used as blank, to avoid external endotoxin interference. All tubs and tips or diluents used to perform this quantification must be endotoxin-free.

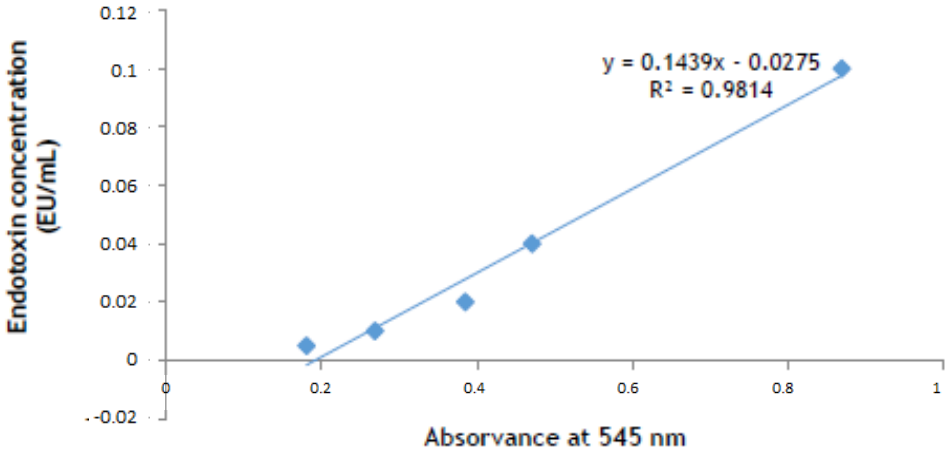

Figure 13- Calibration curve of endotoxins standards (0.01 – 0.1 EU/mL).

3.2.10 Nanoparticle synthesis

The synthesis of the nanoparticles was based on the co-precipitation method previously described [95]. Two solutions were prepared: solution A containing 5 µg de pDNA, 96 µL de $MgCl_2$ (30 mg/mL) and 120 µL of deionized water; solution B containing 255 µL of $NaCO_3$ (42.5 µg/mL), 5 µL of deionized water, 5 µL of gelatin (5 mg/mL) and 5 µL of mannose or galactose (5 mg/mL). Solution A was added dropwise to solution B to form the nanoparticles. The new solution was centrifuged at 13 000 rpm, for 15 min. The pellet containing the pDNA/$MgCO_3$ nanoparticles was washed five times.

3.2.11 Nanoparticles morphology

The nanoparticles morphology was analyzed by two equipments. For the first one, the pellet of nanoparticles was suspended in 40 µL of tungsten 1% and diluted 1:20. 10 µL of the recently formed solution was set in roundly shaped cover-slip and incubated to dry, at room temperature, overnight. On the following day, the nanoparticles are coated with gold using an Emitech K550 sputter coater (London, England) and analyzed by scanning electron microscope (SEM) (Hitachi S-2700, Tokyo, Japan), operated at an accelerating voltage of 20 kV with variable magnifications. For the second one, the pellet nanoparticles were suspended in deionized water, sonicated and analyzed by transmission electron microscopy (TEM) (Hitachi, Japan).

3.2.12 Encapsulation Efficiency

After the nanoparticles formulation and centrifugation, the supernatant was recovered. The supernatant corresponds to the unbound pDNA that was not encapsulated by the $MgCO_3$ nanoparticles. The concentration of the unbound pDNA was measured by Ultrospec 3000 UV-

Visible Spectrophotometer (Pharmacia Biotech, Cambridge, England), at 260 nm. Three independent measurements were performed and the components of the nanoparticles without the pDNA were used as blank. The encapsulation efficiency was determined by the following formula:

$$\%EE = \frac{total\ amount\ of\ pDNA - unbound\ pDNA}{total\ amount\ of\ pDNA} \times 100 \quad (1)$$

Similarly, galactose encapsulation efficiency was determined by using the equation above, with pDNA being replaced by galactose. The non-incorporated galactose was determined quantitatively by using the Galactose Colorimetric/Fluorimetric Assay kit (Sigma-Aldrich). In this assay kit, galactose is oxidized resulting in a colorimetric (570 nm)/fluorimetric (λ_{ex} = 535nm/ λ_{ex} = 587 nm) product, proportional to the galactose present. In this work, galactose has been quantified by the colorimetric detection, measuring the absorbance at 570 nm.

3.2.13 Nanoparticles Size and Zeta (ζ) Potential

The average size and the surface charges (ζ potential) of the nanoparticles were determined at 25 ºC, using a Zetasizer Nano ZS and a zeta dip cell. Determination of the nanoparticles size was made by dynamic light scattering (DLS) using a He-Ne laser 633 nm with non-invasive backscatter optics (NIBS). For the ζ potential determination, electrophoretic light scattering using a patented laser interferometric technique named M3-PALS (Phase analysis Light Scattering) was applied. It was used the Malvern Zetasizer software v6.34. The average values of size and ζ potential were determined with the obtained data from three measurements and the respective standard deviations (SD), presented as ± SD.

3.2.14 Cell Culture

HeLa cells were cultured in Dulbecco's Modified Eagle Medium (DMEM)-High Glucose Medium (Sigma-Aldrich, St. Louis, MO, USA) supplemented with 10% (v:v) of fetal bovine serum (FBS) and a mixture of penicillin (100 µg/mL) and streptomycin (100 µg/mL). Fibroblasts were cultured in DMEM-F12, suplemented with 10% of FBS and a mixture of penicillin (100 µg/mL) and streptomycin (100 µg/mL). All cells were grown at 37 ºC in a humidified atmosphere with 5% of CO_2 in air.

3.2.15 Cell Cytotoxicity

Before cell seeding, the plates were UV irradiated for 30 min. Human fibroblast cells were plated at confluency in 96 well plate, with 2×10^4 per well, respectively, at 37 ºC in 5% CO_2 humidified atmosphere, for 24 and 48h. . The pDNA nanoparticles were applied to a 96-well plate (Nunc.) After incubation, the redox activity was assessed through the reduction of the 3-[4,5-dimethyl-thiazol-2-yl]-2,5-diphenyltetrazolium bromide (MTT). 100 µL of MTT dye solution (0.05 mg/mL in Krebs) was added to each well, followed by incubation for 2 h at 37 ºC, in a 5% CO_2 atmosphere. The medium was aspirated and the cells were treated with 50 µL

of isopropanol/HCl (0.04 N) for 30 min. Absorbance at 570 nm was measured using a Biorad Microplate Reader Benchmark. The spectrophotometer was calibrated to zero absorbance using the culture medium without cells. The relative cell viability (%) related to control wells was calculated by:

$$\frac{[A]test}{[A]control} \times 100 \quad (2)$$

where [A] test is the absorbance of the test sample and [A]control is the absorbance of the control sample. All the experiments were repeated three times. The statistical analysis of experimental data used the Student´s t-test and the results were presented as mean ± SD. Statistical significance was accepted at a level of $p < 0.05$.

3.2.16 FITC-pDNA staining

For the pDNA staining with fluorescein isothiocyanate isomer I (FITC), 71 µg of labeling buffer and 2 µg of FITC were added at 5 µg of pDNA and incubated for 4h. Then, 1 volume of NaCl 3 M and 2.5 volumes of ethanol 100% were added to the solution and incubated at -20ºC overnight. The solution was centrifuged during 30 min, at 12 000g and 4ºC and washed two times with ethanol 75% (centrifugation during 5 min at 12 000g and 4ºC). The pellet with the FITC-pDNA was used for the nanoparticles preparation.

3.2.17 Transfection

Cell live imaging

HeLa cells were cultured up to 80-90% confluence and trypsinized. After the cells were ressuspended in new complete medium, a small volume was seeded in a µ-slide of 8 wells. After 24h, the complete medium was substituted by medium without antibiotic and FBS and the nucleus stained with Hoescht 33342 1:1000, for 20 min in the dark. The µ-slide of 8 wells was transfer to the confocal microscope, containing a camera to maintain 37ºC and 5% of CO_2, and the pDNA-FITC/$MgCO_3$ nanoparticles were injected and imagens of z-stacks were captured (20 min each) during 6h of transfection.

Chapter IV – Results and Discussion

4.1 HPV E6/E7^{MUT} plasmid DNA purification

4.1.1 Epoxy monolith modification

With the aim of understanding the influence of different functional groups immobilized in epoxy monoliths used in the present work, a screening was performed to evaluate the chromatographic behavior of a pre-purified pDNA sample in different epoxy monoliths (non-modified, modified with the 2-allyloxyethanol spacer arm, modified with arginine amino acid and modified with the 2-allyloxyethanol spacer arm and arginine). Thus, two chromatographic strategies were performed on each monolith: to analyze their behavior under hydrophobic conditions, a decreasing linear gradient from 3 to 0 M of $(NH_4)_2SO_4$ in Tris-EDTA, pH 8, was implemented and to analyze their behavior under ionic conditions, an increasing linear gradient from 0 to 3 M NaCl in Tris-EDTA, pH 8, was conducted. Each linear gradient was performed during 15 min.

Analyzing the retention time (rt) values summarized in table 4, the non-modified epoxy monolith retained the pDNA only under hydrophobic elution conditions, eluting at around 11 min. This chromatographic behavior might be justified by the interaction of the exposed hydrophobic bases of nucleic acids and the hydrophobic epoxy groups, in the presence of high $(NH_4)_2SO_4$ concentrations [103]. After, it was evaluated the addition of the 2-allyloxyethanol spacer arm in the epoxy monolith, that retained the pDNA also only under hydrophobic conditions, with a rt of 12 min, meaning a slight increase on the ligand hydrophobicity. The epoxy monolith with immobilized arginine amino acids had an entirely different chromatographic behavior, since only retained the pDNA under ionic elution conditions, being eluted after 10 min. At last, the arginine monolith with the 2-allyloxyethanol spacer arm had a lower rt (8.6 min and only under ionic conditions) comparing to the arginine monolith.

Table 4 - Evaluation of the retention time of four epoxy monoliths (non-modified, modified with the 2-allyloxyethanol spacer arm, modified with arginine amino acid and modified with the 2-allyloxyethanol spacer arm and arginine), under hydrophobic and ionic elution conditions.

	Hydrophobic condition	Ionic condition
Non-modified	10.7	—
With spacer arm	12	—
Arginine	—	10
Arginine with spacer arm	—	8.6

This might be because of the mild influence of the spacer arm on the pDNA interactions due to its electronegative feature. A similar behavior was already described in previous studies with arginine and agmatine monoliths [75, 104]. The agmatine ligand is a neurotransmitter derived from the decarboxylation of arginine amino acid. The absence of the negative carboxyl group favored multiple non-covalent interactions that result in higher pDNA retention and the need of higher NaCl concentrations (>1.8 M) for the pDNA elution [104], comparing to the arginine ligand (795 mM NaCl) [75]. The arginine monolith with spacer arm was later characterized and explored for the sc pDNA purification.

4.1.2 Dynamic binding capacity

The DBC is an important factor to characterize the chromatographic support. It is already described that monoliths have higher binding capacity when compared to the conventional chromatographic supports [73, 75, 105]. These last ones are designed with small size pores that cannot handle large molecules, such as pDNA [65].

For instance, Eon-Duval and coworkers demonstrated that a DEAE column has a dynamic capacity of 3 mg/mL [106] and Ongkudon and coworkers showed that polymethacrylate conical monolith has a DBC of 21.54 mg/mL [107]. Moreover, some latest results also shown that methacrylate monolithic supports exhibit DBC up to 8 mg/mL [108]. Recently, Amorim and coworkers showed that the capacity of L-histidine monolith (6.24 mg/mL) is 29-fold higher than that of the conventional histidine–agarose matrix (0.217 mg/mL) at 50% of breakthrough curves [109].

Hence, the arginine monolith with spacer arm was characterized in terms of DBC and was compared to the conventional agarose-based matrix and arginine monolith. Breakthrough experiments were performed at 1 mL/min, with 0.05 mg/mL of the pre-purified pDNA (figure 14). The column was equilibrated with Tris-EDTA, pH 8.0 and then overloaded with the pDNA sample. To determine the DBC of the arginine monolith with spacer arm, it was calculated the amount of pDNA per mL of support at 10%, 50% and 100% breakthrough curve. After, the pDNA was eluted with 1 M NaCl in Tris-EDTA, pH 8.0 and the monolith was regenerated with 0.5 M NaOH solution.

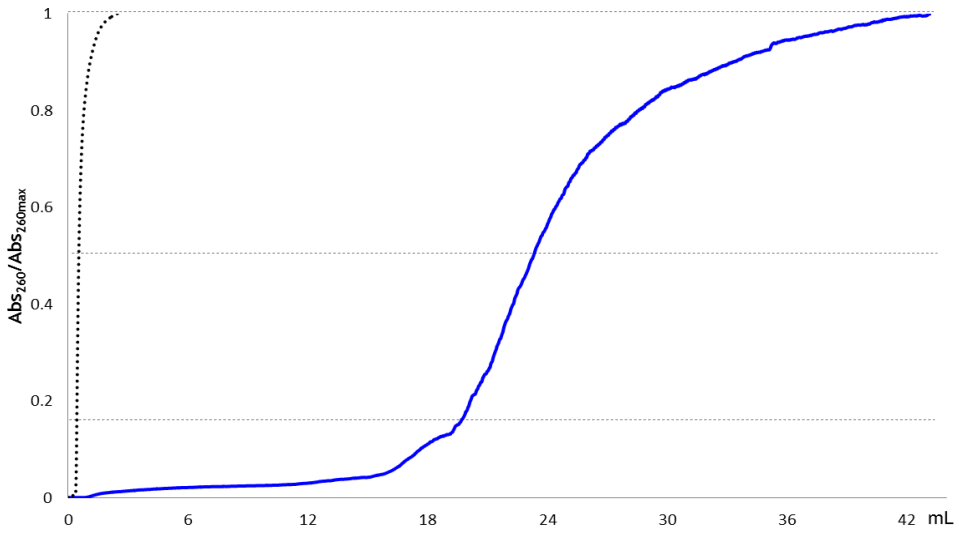

Figure 14 - Breakthrough curve (continuous line) **and void volume** (dashed line) **of arginine monolith with spacer arm.** pDNA solution (0.05 mg/mL) was loaded at 1 mL/min.

The DBC at 10% of breakthrough curve was 2.53 mg/mL, which is much higher than the 0.133 mg/mL of the conventional support of arginine agarose but lower than the 3.55 mg/mL of the arginine monolith [75]. The difference between the DBC of the arginine monolith and the arginine monolith with spacer arm can be due to the lower amount of available ligands in the last one or to the electronegativity of the 2-allyloxyethanol spacer arm, which may promote some repulsion by the pDNA phosphate groups under ionic conditions.

The conventional agarose-based matrix does not have channels like the monolithic support, thus the pDNA molecules only interact with the functional groups that are at the bead surface which represents a lower surface area.

On the other hand, monoliths have become the chromatographic support of choice for the purification of sc pDNA, since they are capable of separating large biomolecules, such as pDNA, they enable a fast separation with a reduced retention time, allowing the pDNA integrity maintenance. Monoliths have the great advantage of higher binding capacity comparing to conventional supports [65, 73, 110]. In fact, the DBC of the arginine monolith with spacer arm was 19-fold higher than the DBC of the arginine agarose-based support at 10% breakthrough. For this reason, the arginine monolith with spacer arm presented in this work can be a promising affinity chromatographic support.

4.1.3 Separation of HPV E6/E7^{MUT} plasmid DNA isoforms

The purification strategy explored initially in the present work, for the arginine monolith with spacer arm, had already been described by our research group for HPV E6/E7 pDNA purification in the arginine monolith, based on increasing stepwise gradient of NaCl (ionic elution conditions) [75]. For a first evaluation of the selectivity, several experiments were performed to study the elution/retention chromatographic behavior of the arginine monolith with spacer arm, towards finding the ideal conditions to separate the pDNA isoforms. All the experiments were performed at room temperature. First, the monolith was equilibrated with 584 mM NaCl in Tris-EDTA, pH 8.0, at 1 mL/min. After injection of 200 µl of the pDNA sample resulting from alkaline lysis and pre-purification with *Qiagen Plasmid Purification Maxi Kit* from *Qiagen*, the unbound species were eluted. Then, the ionic strength was increase to 1 M NaCl in Tris-EDTA, pH 8.0, to elute the bound species (figure 15 A). The agarose gel electrophoresis showed that the linear pDNA started to elute in the first peak, but some amount still elute in the second peak, along with the sc pDNA (figure 15 A, lane 1 and 2, respectively). Thus, the concentration of NaCl on the equilibrium step was increased, aiming the total elution of the linear pDNA on the first peak. The monolith was equilibrated with 596 mM NaCl in Tris-EDTA, pH 8.0, and after the elution of unbound species the ionic strength was increased to 1 M NaCl in Tris-EDTA, pH 8.0, caused the elution of the bound species (figure 15 B). As shown at figure 15 B, the sc pDNA started to elute in the first peak with the linear isoform, which continues to have an amount that elutes in the second peak. A higher NaCl concentration (620 mM) was also tested in the equilibrium step but the agarose gel electrophoresis presented on figure 15 C reveals that the linear and the sc pDNA were eluted in both peaks, showing that the desired selectivity was not achieved only by the manipulation of NaCl concentrations in the equilibrium step.

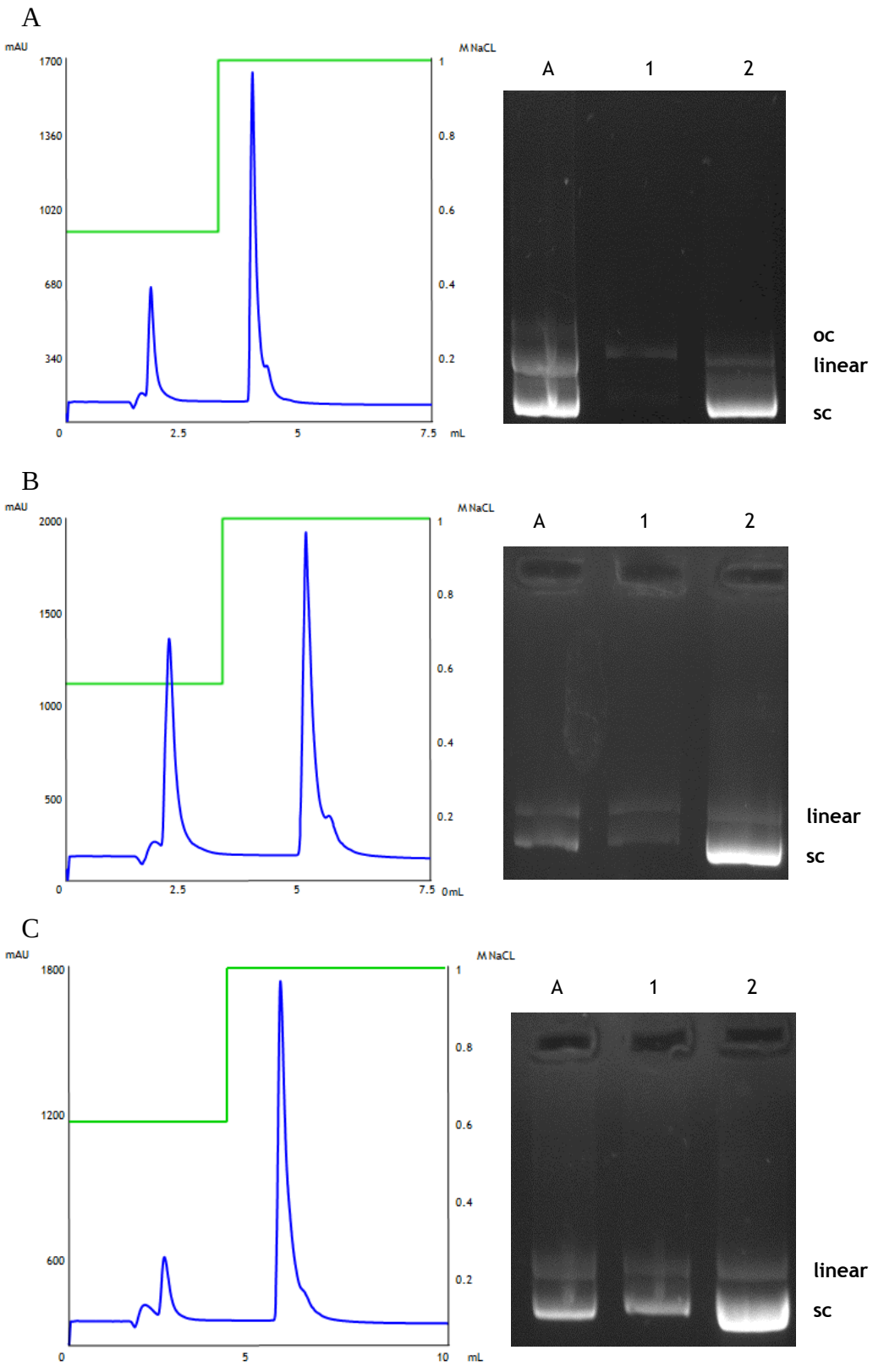

Figure 15 – Chromatographic profile of the pre-purified pDNA sample in the arginine monolith with spacer arm, at a laboratorial scale, using a stepwise gradient of 584 (A), 596 (B) and 620 (C) mM in the equilibration steps and 1 M NaCl in Tris- EDTA, pH 8.0 in the elution steps, 1 mL/min. Injection volume: 200 µL of pre-purified pDNA (oc + linear + sc). Agarose gel electrophoresis of the recovered peaks. Lane A - pDNA sample; lane 1 and 2 - peak 1 and peak 2, respectively.

According to Almeida and coworkers, the pH manipulation can improve the selectivity of arginine ligand and the sc pDNA recovery yield [111]. Therefore, the pH buffer was change to 7.0. After several experiments by manipulating the NaCl concentration on the equilibrium step at pH 7.0, the elution conditions that seem to be the best are described below. The monolith was equilibrated with 680 mM NaCl in Tris-EDTA, pH 7.0. After the injection of 200 µl of pre-purified pDNA sample onto the column, the unbound species were eluted in the flow-through. Thereafter, the ionic strength was increase to 1 M NaCl in Tris-EDTA, pH 7.0 and a second peak was obtained with the bound species, at 1 mL/min (figure 16 A). The agarose gel electrophoresis confirmed that the linear pDNA elution occurred in the first peak together with a small amount of sc pDNA (figure 16 B, lane 2). The second peak contained the sc pDNA, totally isolated (figure 16 B, lane 3). In this way, the total recovery of the sc pDNA must be sacrificed, in favor of obtaining the desired isoform with the required purity at the second peak.

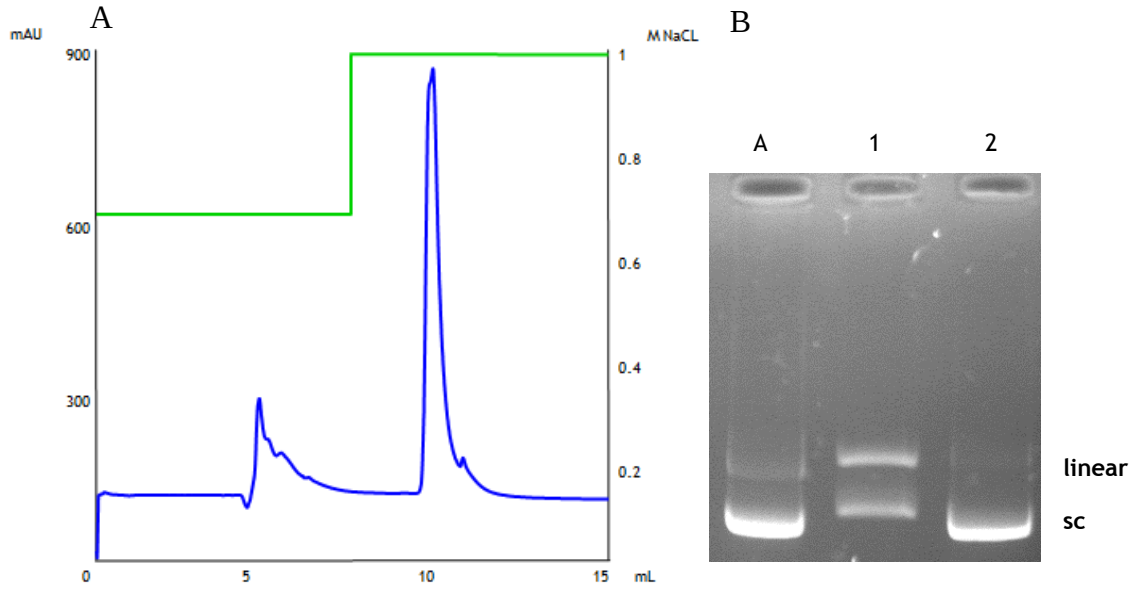

Figure 16 – (A) Chromatographic profile of the pre-purified pDNA sample in the arginine monolith with spacer arm, at a laboratorial scale, using a stepwise gradient of 680 mM and 1 M NaCl in Tris-EDTA, pH 7.0, 1 mL/min. Injection volume: 200 µL of pre-purified pDNA (oc + linear + sc). (B) Agarose gel electrophoresis of the recovered peaks. Lane A - pDNA sample; lane 1 and 2 - peak 1 and peak 2, respectively.

4.1.4 Purification of HPV E6/E7^{MUT} plasmid DNA from a complex *E. coli* lysate sample

The previous results indicate that the immobilized arginine in the monolith with spacer arm recognizes specifically the sc pDNA isoform. For the purpose of separating the sc pDNA from a lysate sample (other pDNA isoforms, RNA, gDNA, proteins and endotoxins), different strategies can be explored such as the use of competitive ligand or the manipulation of pH, ionic strength or polarity, depending on the matrix and the characteristics of the biomolecule

[57]. Thereby, the results previously described were taken into account to start the experiments on the purification of sc pDNA from a lysate sample, at a laboratorial scale.

The first experiment was based on the ideal elution conditions that allowed the isolation of the sc pDNA isoform from the pre-purified pDNA sample. Thus, the monolith was equilibrated with 680 mM NaCl in Tris-EDTA, pH 7.0, at 1 mL/min. After injection of 200 µL of lysate sample, the unbound species were eluted in the flow-through. To elute the bound species, the ionic strength was increased to 1 M NaCl in Tris-EDTA, pH 7.0. The correspondent chromatogram and agarose gel electrophoresis of each peak are presented on figure 17 A.

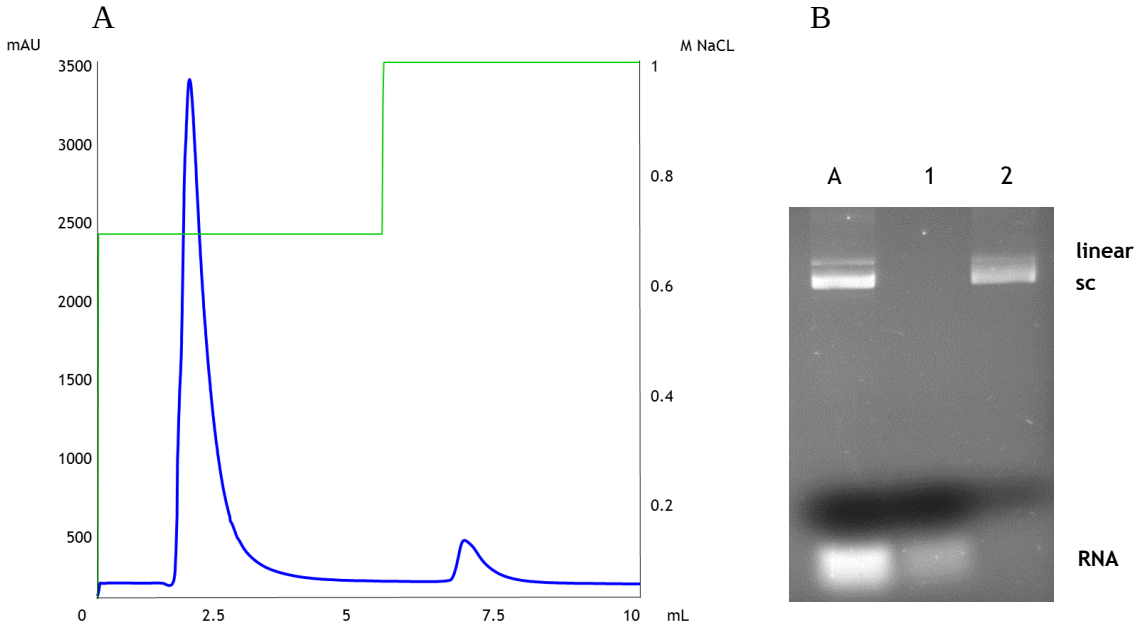

Figure 17 – (A) Chromatographic profile of the *E. coli* lysate sample in arginine monolith with spacer arm, at a laboratorial scale, using a stepwise gradient of 680 mM and 1 M NaCl in Tris-EDTA, pH 7.0. Injection volume: 200 µL of lysate sample. (B) Agarose gel electrophoresis of the recovered peaks. Lane A - lysate sample; lane 1 and 2 - peak 1and 2, respectively.

Figure 17 B revealed that only the RNA eluted in the first peak and all of the different plasmid isoforms eluted in the second one. Although RNA molecules are negatively charged and single stranded, they have low molecular weight, comparing to pDNA [42]. In addition, this result also shows that the presence of other nucleic acids can alter the binding/elution behavior of the pDNA isoforms, which were eluted together in the second peak. Thus, more experiments were performed, adding an additional step and manipulating the NaCl concentration. Considering that the equilibration step with 680 mM NaCl in Tris-EDTA, pH 7.0 allowed the total elimination of the RNA in the flow-through, this step was maintained. Then, two elution steps were performed by increasing the NaCl concentration to separate the retained species (710 mM and 1 M NaCl in Tris-EDTA, pH 7.0). The agarose gel electrophoresis revealed that both linear and sc pDNA isoforms were eluted in both peaks (figure 18 A).

Since there was no selectivity with previous elution steps, different concentrations of NaCl were explored in the first elution step. For instance, it was used a concentration of 800 mM NaCl in Tris-EDTA, pH 7.0, but, as it is presented on figure 18 B, although the recovery of the sc pDNA in the last peak is sacrificed, it was not possible to obtain the desired conformation totally purified. These results allow to conclude that the strategy by manipulation of NaCl concentration in the elution step was unable to selectively separate the sc pDNA from the other isoforms.

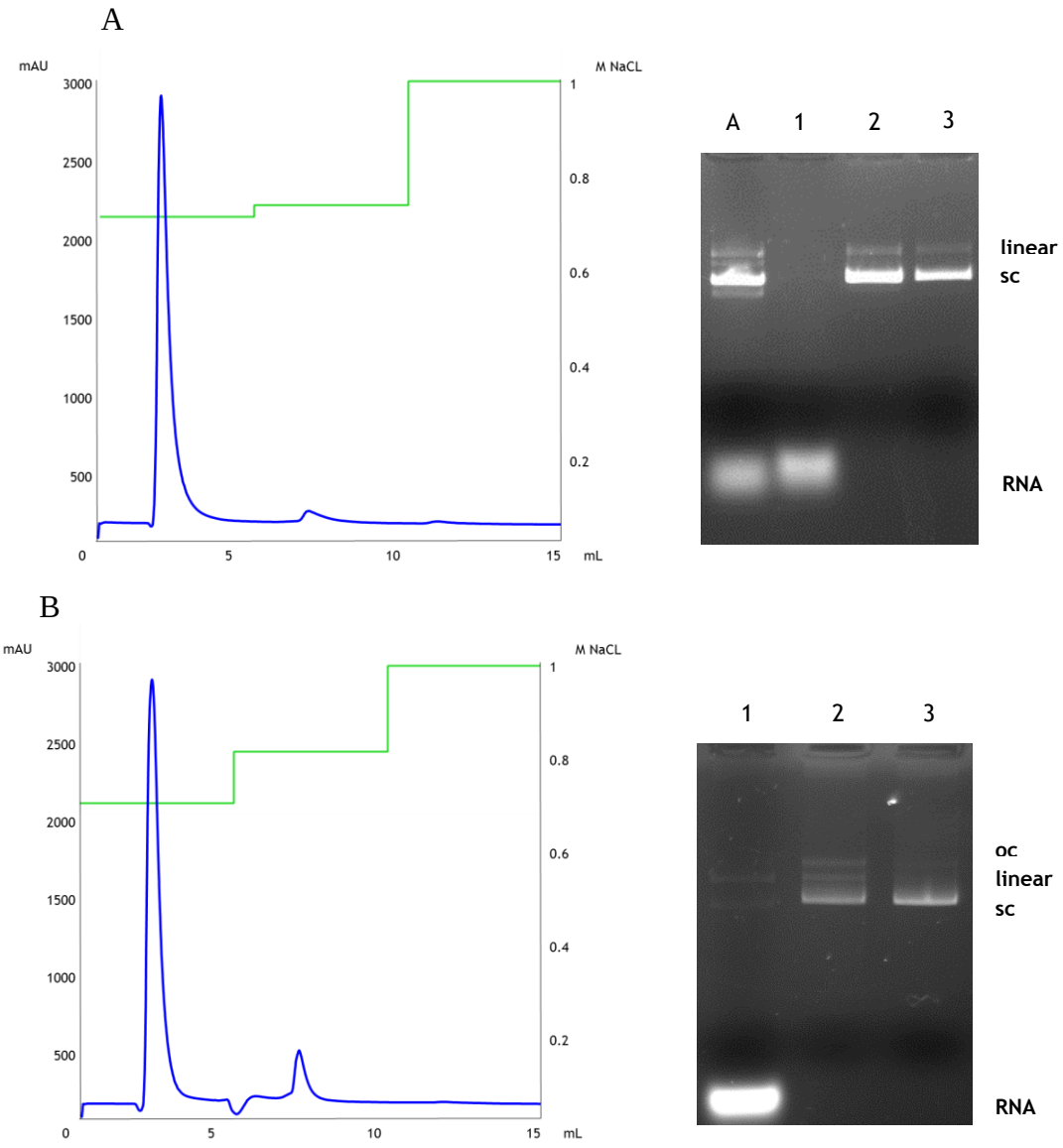

Figure 18 - Chromatographic profile of the *E. coli* lysate sample in arginine monolith with spacer arm, at a laboratorial scale, using a stepwise gradient of 680 mM in the equilibrium steps, 710 mM (A), 800 (B) in the first elution steps and 1 mM NaCl in Tris-EDTA, pH 7.0 in the second elution steps. Injection volume: 200 µL of lysate sample. Agarose gel electrophoresis of the recovered peaks. Lane A - lysate sample; lane 1, 2 and 3 - peak 1, 2and 3, respectively.

As mentioned above, the elution strategy can be through the addition of a competitive agent, where the elution buffer has the same pH, ionic strength and polarity as the equilibrium

buffer. The competing agent can bind to the retained biomolecule or to the immobilized ligand, thus preventing interactions between the biomolecule and the ligand. This allows a biospecific elution, it being more selective [112]. In fact, Pereira and coworkers have already demonstrated the successful application of arginine as a competing agent on the purification of pre-miR-29 [113]. Bearing this in mind, further experiments were carried out, using a competitive elution strategy, always maintaining the equilibration step to eliminate the RNA. Arginine was used as a competing agent on the elution buffer and several concentrations were tested (10 mM, 5 mM, 2 mM, 1 mM, 0.5 mM and 0.01 mM). All the experiments showed an identical chromatographic behavior as the chromatographic profile presented on figure 19 A, where the second step was executed with the equilibrium buffer supplemented with 0.01 mM arginine and the third step was performed with 1 M NaCl in Tris-EDTA, pH 7.0. The correspondent electrophoresis revealed that the majority of the sc pDNA was eluted in the second step, along with the other isoforms (figure 19 B).

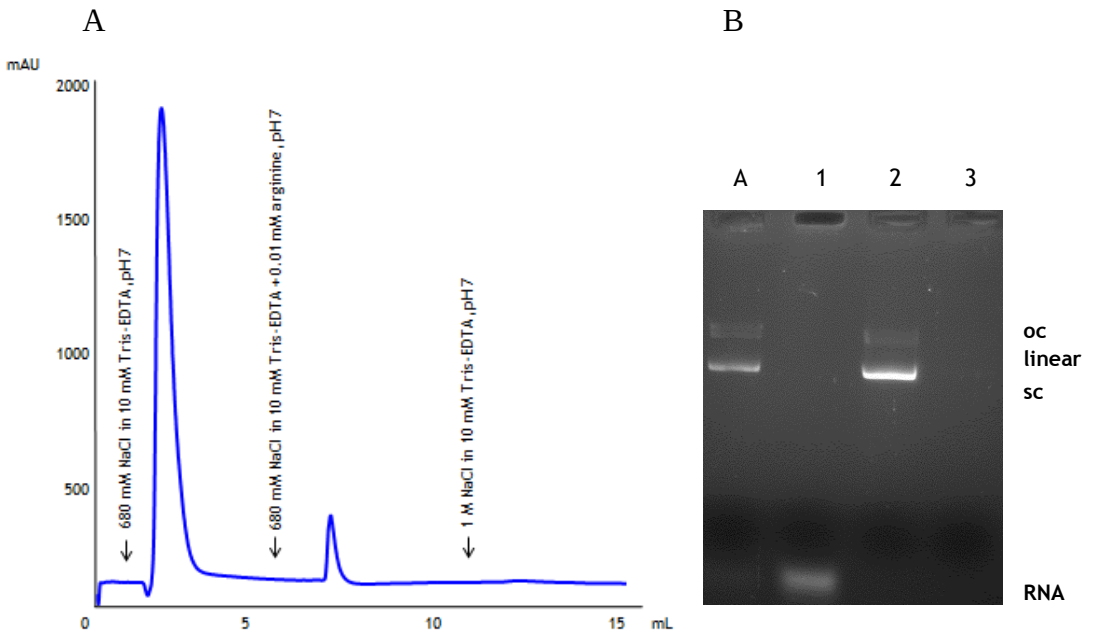

Figure 19 - (A) Chromatographic profile of the *E. coli* lysate sample in arginine monolith with spacer arm, at a laboratorial scale, using a stepwise gradient of 680 mM, 680 mM + 0.01 mM arginine and 1 M NaCl in Tris-EDTA, pH 7.0. Injection volume: 200 µL of lysate sample. (B) Agarose gel electrophoresis of the recovered peaks. Lane A - lysate sample; lane 1, 2 and 3 - peak 1, 2and 3, respectively.

This competitive elution is based on the interaction between the retained biomolecule (pDNA) and the competing agent (free arginine). Hence, in the presence of free arginine in the elution buffer, the target biomolecule is no longer retained, being eluted. The low selectivity of this strategy might be due to the fact that the arginine positive charge promotes preferential binding of pDNA with free arginine present in the elution buffer, through electrostatic interactions [114].

As it was previously referred, the pH manipulation can improve the selectivity of arginine ligand and the sc pDNA recovery yield [111]. Therefore, other strategy to explore in the purification of the sc pDNA from *E. coli* lysate was the pH variation in the elution buffer (9, 8, 7.5, 7.3 and 6.5). This experiments demonstrated that the higher the pH, the lower the retention, since there is a weaker ionic interaction (data not shown). Considering that the pKa of arginine is 12, high pH leads to less effectiveness of the arginine positive charges, causing a weaker interaction with the pDNA.

The condition that showed the best outcome was with pH 7.5. Likewise, the equilibration step with 680 mM NaCl in Tris-EDTA, pH 7.0, was also maintained on these experiments, since it allows the RNA elution on the flow-through. Then, the elution buffer was changed to 650 mM and 1 M of NaCl in Tris-EDTA, pH 7.5, resulting in the elution of two peaks (figure 20 A). The analysis of the respective agarose gel electrophoresis proved that this strategy enables the selective separation of non-functional plasmid isoforms in the second peak and the recovery of sc pDNA almost isolated in the third peak (figure 20 B, lane 2 and 3, respectively).

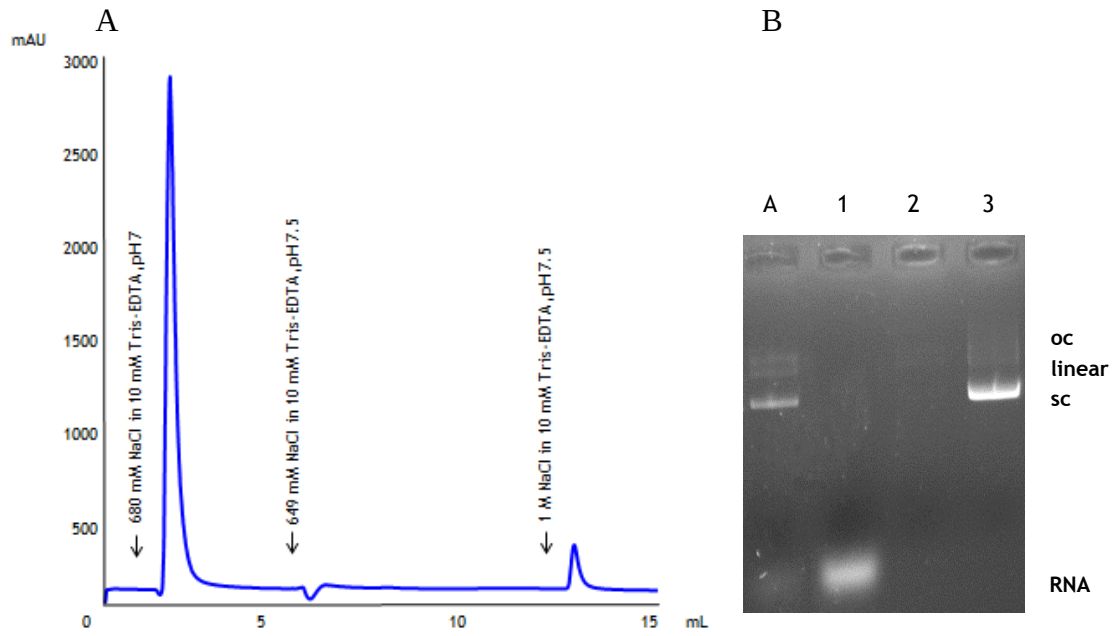

Figure 20 - (A) Chromatographic profile of the *E. coli* lysate sample in arginine monolith with spacer arm, at a laboratorial scale, using a stepwise gradient of 680 mM in Tris-EDTA, pH 7.0, 649 mM and 1 M NaCl in Tris-EDTA, pH 7.5. Injection volume: 200 µL of lysate sample. (B) Agarose gel electrophoresis of the recovered peaks. Lane A - lysate sample; lane 1, 2 and 3 - peak 1, 2and 3, respectively.

The results described earlier indicate that the differential interactions between nucleic acids of the lysate sample and the arginine monolith with spacer arm comply with what was previously described [75, 111]. The predominant electrostatic interactions, mostly between the arginine positive charges and the negative phosphate groups of the nucleic acids, are due to the fact that the working pH is lower that the pKa of arginine (12) [115]. These

interactions can be weakened by competition with the ions of the NaCl buffer, increasing its concentration and thus reducing the effective net charge between the ligand and lower affinity species [116]. This is why RNA was eluted in the flow-through of the equilibration buffer, since it has less interaction points when compared to pDNA under these equilibrium conditions. Moreover, the specific recognition of the sc pDNA isoform in relation to other isoforms might be because of the additional non-covalent interactions with the arginine ligand, such as cation-π interactions, bifurcate hydrogen bonds and hydrogen-π interactions, mainly with the more exposed bases of this conformation caused by the supercoiled phenomena [56, 117]. Consequently, the slight increase of the buffer pH, along with the adjustment of the ionic strength, allowed the elution of species with lower affinity (oc and linear pDNA isoforms) and the isolation of the sc pDNA in the last peak.

4.1.5 Recovery and purity quantification of the recovered peaks

The sc pDNA purified fractions obtained from the optimized chromatographic elution strategy were analyzed in terms of purity and recovery yield, by CIMac™ pDNA analytical column, according to the method previously described [77]. First, the analytical column was equilibrated with 600 mM of NaCl in 200 mM Tris-HCl buffer (pH 8.0). After, 20 µL of the sample recovered from the peak of interest was injected onto the column and a linear gradient from 600 mM to 700 mM of NaCl was applied, during 10 min, eluting the retained pDNA isoforms.

The purity degree was determined by the ratio between the sc pDNA peak area and the total peak area in the analytical chromatogram, it being 93.3%. This value supports the fact that arginine monolith with spacer arm can highly purify sc pDNA from a lysate sample. The recovery yield was calculated through the ration between the recovered sc pDNA concentration and the sc pDNA concentration from the lysate sample, it being almost 72%. This value can be due to the sc plasmid loss during its recuperation, concentration and desalting steps [73, 75]. Though this recovery yield is lower than the 86% obtained with the arginine monolith [75], it is satisfactory, comparing to other chromatographic strategies, like the 62% of recovery yield obtained with anion exchange [118] and the triplex affinity chromatography [119], as well as the 70% attained from hydrophobic interaction chromatography [101].

4.1.6 Preparative chromatography

The applicability of arginine monolith with spacer arm was also explored in the purification of sc pDNA isoform at a preparative scale (figure 21 A). The elution conditions were conducted in order to ensure the purity of the final pDNA sample. The column was loaded with 68 mL of lysate sample prepared in the same equilibrium buffer (680 mM NaCl in Tris-EDTA, pH 7.0). The agarose gel electrophoresis revealed that the RNA was eluted throughout the assay,

joined by the oc and linear isoforms elution and lastly the sc plasmid isoform partial elution (figure 21 B).

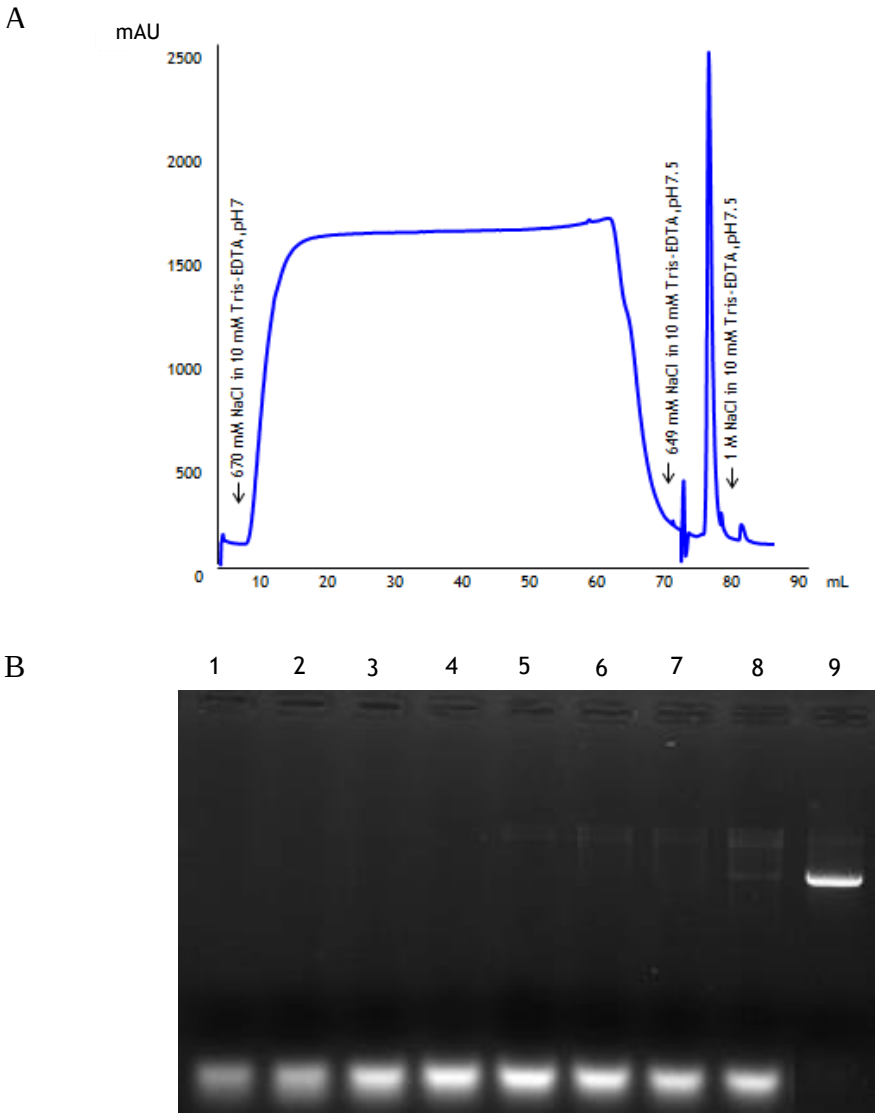

Figure 21 - (A) Chromatographic profile of the E. coli lysate sample in arginine monolith with spacer arm, at a preparative scale under overloading conditions, using a stepwise gradient of 670 mM in Tris-EDTA, pH 7.0, 649 mM and 1 M NaCl in Tris-EDTA, pH 7.5. (B) Respective agarose gel electrophoresis. Lane 1-8 - peak 1; lane 9 - peak 2, respectively.

This behavior is similar to the one observed in the laboratorial scale assay, suggesting that the preferential retention of sc pDNA also occurred in overloaded conditions. After the column loading, two steps were performed (with 649 mM and 1 M NaCl in Tris-EDTA, pH 7.5) to elute the bound species. Figure 21 shows the recovery of sc pDNA in the first elution step, almost free of other plasmid isoforms. In this approach, 0.83 mg of pDNA/mL of column were recovered, with a purity higher than the result obtained in the laboratorial approach (98.5% and 93.3%, respectively). These results indicate that the elution strategy applied on the preparative approach is more suitable to obtain the required purity of sc pDNA, although it is

not possible to load higher amount of lysate sample without compromising the sc pDNA recovery.

4.1.7 Host impurities assessment in the purified sc pDNA

To apply the sc HPV-16 E6/E7^{MUT} pDNA vaccine pharmaceutically, it must be obtained from a complex *E. coli* lysate sample and the impurities elimination must be assured, following the regulatory agency specifications: sample homogeneity higher than 97% supercoiled, proteins and RNA undetectable by micro-BCA method and 0.8% agarose gel electrophoresis, respectively, gDNA under 2 µg/mg plasmid by PCR and endotoxins under 0.1 EU/ng plasmid by LAL assay (table 5) [60, 120].

Table 5 - Regulatory agency specifications (adapted from [60, 120]).

Impurities and homogeneity	Criteria
Homogeneity	>97% sc
Proteins	Undetectable
RNA	Undetectable
gDNA	<2 µg/mg
Endotoxins	<0.1 EU/µg pDNA

To reduce pathogenic effects and adverse reactions, the pDNA for therapeutic application should be free from contaminants and host impurities [121]. Regarding the content of protein, is must be undetectable, since they can cause immune responses, like anaphylactic shock or autoimmune diseases, or induce biological reactions due to the production of cytokines, hormones and/or antibodies [122, 123]. Hence, the regulatory agencies define that proteins should be undetectable in the sc pDNA sample (table 5). The protein content was assessed by the micro-BCA assay, already described on chapter 3.2.7. The results shown in table 6 present that the protein content of the lysate sample and the pDNA sample was undetectable, either at the laboratorial or preparative scale, being in agreement with the requirements of the regulatory agencies. These results suggest that the clarification step with 2.5 M of ammonium sulfate in the end of the lysis procedure was effective in the removal of proteins.

Another parameter that must be measured is the gDNA, because some of its fragments can encode an oncogene that can integrate the cell genome after transfection, possibly causing tumor formation [122]. The quantification of gDNA was obtained with real-time PCR. As presented in table 6, the gDNA amount at the laboratorial scale was initially 9.980 ng/µg of pDNA and considerably reduced to 0.090 ng/µg of pDNA. At the preparative scale, the initial gDNA amount was 7.320 ng/µg of pDNA and reduced to 0.680 ng/µg of pDNA. Both values are below the limit imposed by the regulatory agencies (2 µg/mg of pDNA).

Endotoxins are highly negatively charged lipopolysaccharides (LPS) that constitutes the cell wall of gram negative bacteria, such as *E. coli* [122]. They can cause strong biological effects, including activation of the immune system, stimulation of cytokines overproduction, fever, induction of endotoxin shock, tissue injury and ultimately death [122, 124, 125]. Endotoxins assessment was performed by the LAL endotoxin assay kit. Endotoxins were reduced from the initial value of 0.434 EU/µg of pDNA in the lysate sample to 0.011 EU/µg of pDNA, at the laboratorial scale. Regarding the preparative scale, endotoxins were also significantly reduced from 5.402 EU/µg of pDNA to 0.003 EU/µg of pDNA. Both values are in agreement with the limits of the regulatory agencies.

Table 6- Protein, gDNA and endotoxins measurement in the sc pDNA recovered fraction from the laboratorial and preparative chromatography approaches.

	Sample	Proteins (mg/mL)	gDNA		Endotoxins	
			(µg/mL)	(ng/µg pDNA)	(EU/mL)	(EU/µg pDNA)
Laboratorial chromatography	Lysate sample	Undetectable	0.649	9.980	28.198	0.434
	pDNA	Undetectable	0.004	0.090	0.539	0.011
Preparative chromatography	Lysate sample	Undetectable	0.038	7.320	28.141	5.402
	pDNA	Undetectable	0.054	0.680	0.264	0.003

4.2 Nanotechnology

4.2.1 $MgCO_3$ Nanoparticles synthesis

The nanoparticles were synthesized by the co-precipitation method, where the solution A with $MgCl_2$ and pDNA is added to the solution B with $CaCO_3$, gelatin and the functionalization compound (mannose or galactose). This creates a precipitate – the nanoparticles - that can be easily recovered by centrifugation.

$$Mg Cl_2(aq) + Na_2CO_3\ (aq) \rightarrow \mathbf{MgCO_3\ (s)} + 2NaCl\ (aq) \quad (3)$$

The choice of these materials for the nanoparticles formation is based on the already well described and effective nanoparticles $CaCO_3$ synthesis protocol [95], but the Ca^{2+} ion was substituted by the Mg^{2+} ion, to investigate if the results of transfection and gene delivery can be improved. The use of inorganic nanoparticles, such as carbonates of Ca^{2+} and Mg^{2+}, might eliminate some limitations of the current non-viral genetic vaccine systems, like the inefficiency of activation of the APCs [126]. Moreover, it has been demonstrated that the incorporation of Mg^{2+} into the nanoparticles caused inhibition of particle growth, leading to a remarkably improvement on the DNA cellular uptake [127].

On the other hand, gelatin is a biocompatible and biodegradable polymer, non-toxic and with low immunogenicity. Its use on the nanoparticles synthesis improves their properties: it reduces the nanoparticles size, enhances their stability and ζ potential, thus improving the gene delivery efficiency [98].

The mechanisms of both humoral and cellular immune responses have already been explained. DNA vaccination aims to activate these two responses, by activating the cytotoxic T lymphocytes (CD8+) as well as the T helper cells (CD4+). These cells recognize the MHC-(I and II, respectively)-peptide complex that is presented on APC surface [35]. The major APC is the dendritic cell (DC). Therefore, with the purpose of delivering the HPV-16 E6/E7^{MUT} pDNA vaccine, targeting the DCs seemed to be a promising strategy to enhance the activating of humoral and cellular immune responses.

DCs express on their surface c-type lectin receptors (CLRs) that recognize glycosylated self-antigens or foreign pathogens [128, 129]. This is particularly relevant and useful considering that an approach of DC-targeting vaccine delivery is desired. Thus, the nanoparticles surface was functionalized with mannose or galactose (carbohydrates that are recognize by CLRs) [128, 130]. This selective delivery of the nanoparticles can facilitate binding and endocytosis by the DC.

4.2.2 Cytotoxicity assay

The MTT assay was performed to assess the $MgCO_3$ nanoparticles effect on cell viability. The results revealed a cell viability of 85% ± 0.9 at 24h and 84% ± 1.0 at 48h. This means that these nanoparticles do not have an acute cytotoxic effect.

The components that were later added to the nanoparticles formulation – gelatin, mannose and galactose – are not expected to be cytotoxic, since they were already used on some transfection studies [131, 132].

4.2.3 Encapsulation efficiency

For therapeutic purposes, the formulation of a suitable pDNA delivery system must incorporate a large amount of genetic material. To evaluate the EE parameter, different quantities of pDNA (5 µg, 7.5 µg, 10 µg, 15 µg and 20 µg) were tested for the different systems and are presented in table 7. Either nanoparticles functionalized with mannose or galactose showed a decay of %EE by increasing the pDNA quantity. This may be due to the large size of the plasmid. Moreover, there was a slight decrease on the %EE of the functionalized nanoparticles when comparing to the non-functionalized ones. Other nanoparticles formulations allowed the same or less %EE. For example, $CaCO_3$ nanoparticles only allowed 51-63% EE [95], chitosan–TPP nanoparticles allowed only up to 80% [133] and poly(lactic acid)-poly(ethylene glycol) nanoparticles allowed up to 90% EE [134]. Therefore, the entire %EE was relatively high.

Table 7 – Average %EE of the different pDNA based nanoparticles. Values were calculated with the data obtained from three independent measurements (mean ± SD, n = 3).

System ($MgCO_3$)	% EE
5 µg pDNA/Gelatin	88.4 ± 1.9
5 µg pDNA/Gelatin/Mannose	87.8 ± 0.5
7.5 µg pDNA/Gelatin/Mannose	79.3 ± 8.0
10 µg pDNA/Gelatin/Mannose	70.6 ± 2.3
15 µg pDNA/Gelatin/Mannose	66.3 ± 0.6
20 µg pDNA/Gelatin/Mannose	62.6 ± 1.7
5 µg pDNA/Gelatin/Galactose	86.3 ± 1.8
7.5 µg pDNA/Gelatin/Galactose	77.6 ± 8.4
10 µg pDNA/Gelatin/Galactose	66.9 ± 5.0
15 µg pDNA/Gelatin/Galactose	61.1 ± 1.0
20 µg pDNA/Gelatin/Galactose	57.9 ± 2.7

4.2.4 Galactose Encapsulation Efficiency

The efficiency of the galactose encapsulation was satisfactory and the differences between the studied quantities of pDNA (5 µg or 10 µg) were not notorious. These results are presented in table 8.

Table 8 - Average %EE of galactose of the pDNA based nanoparticles. Values were calculated with the data obtained from three independent measurements (mean ± SD, n = 3).

System ($MgCO_3$)	% Galactose EE
5 µg pDNA/Gelatin/Galactose	78.7 ± 0.9
10 µg pDNA/Gelatin/Galactose	80.1 ± 1.4

4.2.5 Nanoparticles morphology

Scanning Electron Microscopy (SEM) and transmission electron microscopy (TEM) are techniques that rely on the use of a beam of highly energetic electrons to obtain information about the sample, like morphology. SEM and TEM images of the studied nanoparticles are presented on figure 22.

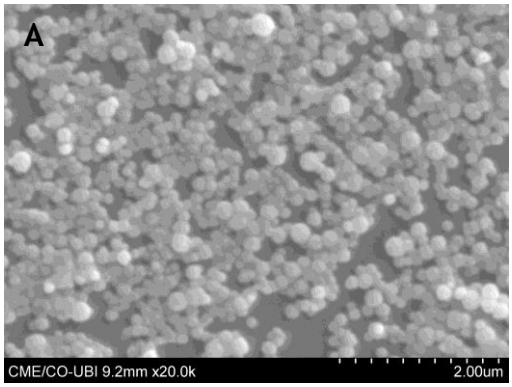
A
CME/CO-UBI 9.2mm x20.0k
2.00um

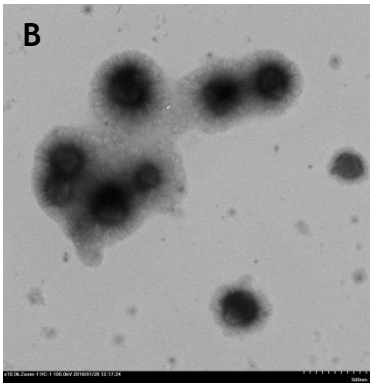
B

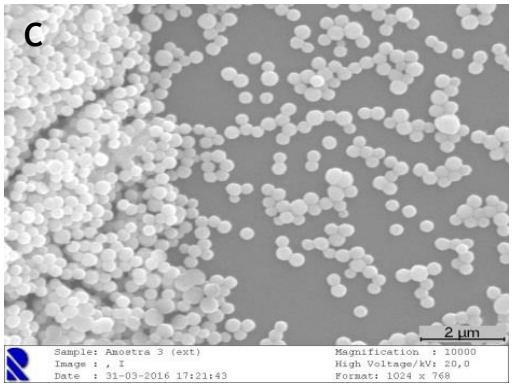
C
2 µm
Sample: Amostra 3 (ext)
Image : , I
Date : 31-03-2016 17:21:43
Magnification : 10000
High Voltage/kV: 20,0
Format: 1024 x 768

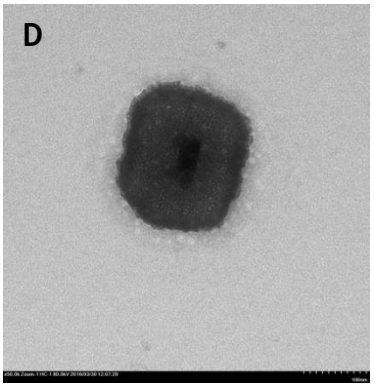
D

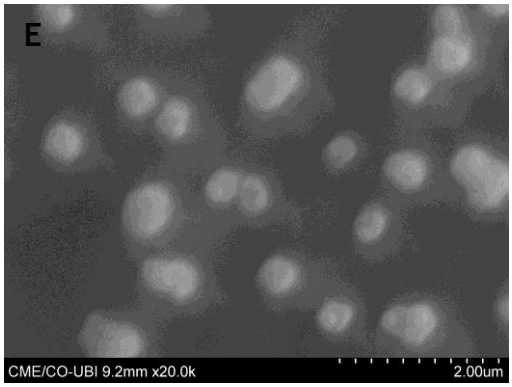
E
CME/CO-UBI 9.2mm x20.0k
2.00um

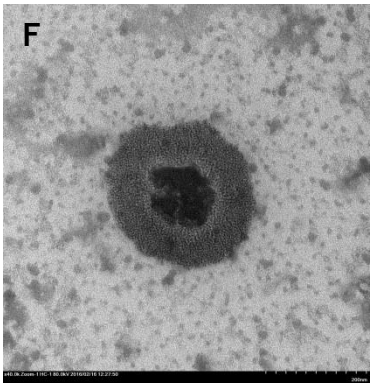
F

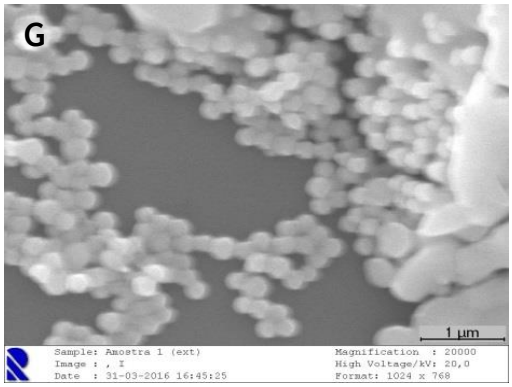
G
1 µm
Sample: Amostra 1 (ext)
Image : , I
Date : 31-03-2016 16:45:25
Magnification : 20000
High Voltage/kV: 20,0
Format: 1024 x 768

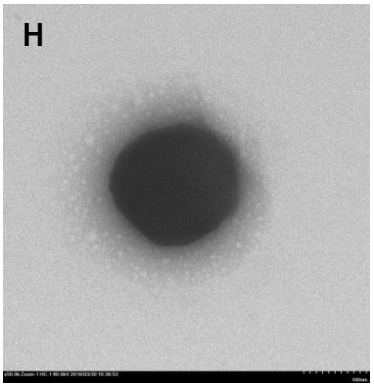
H

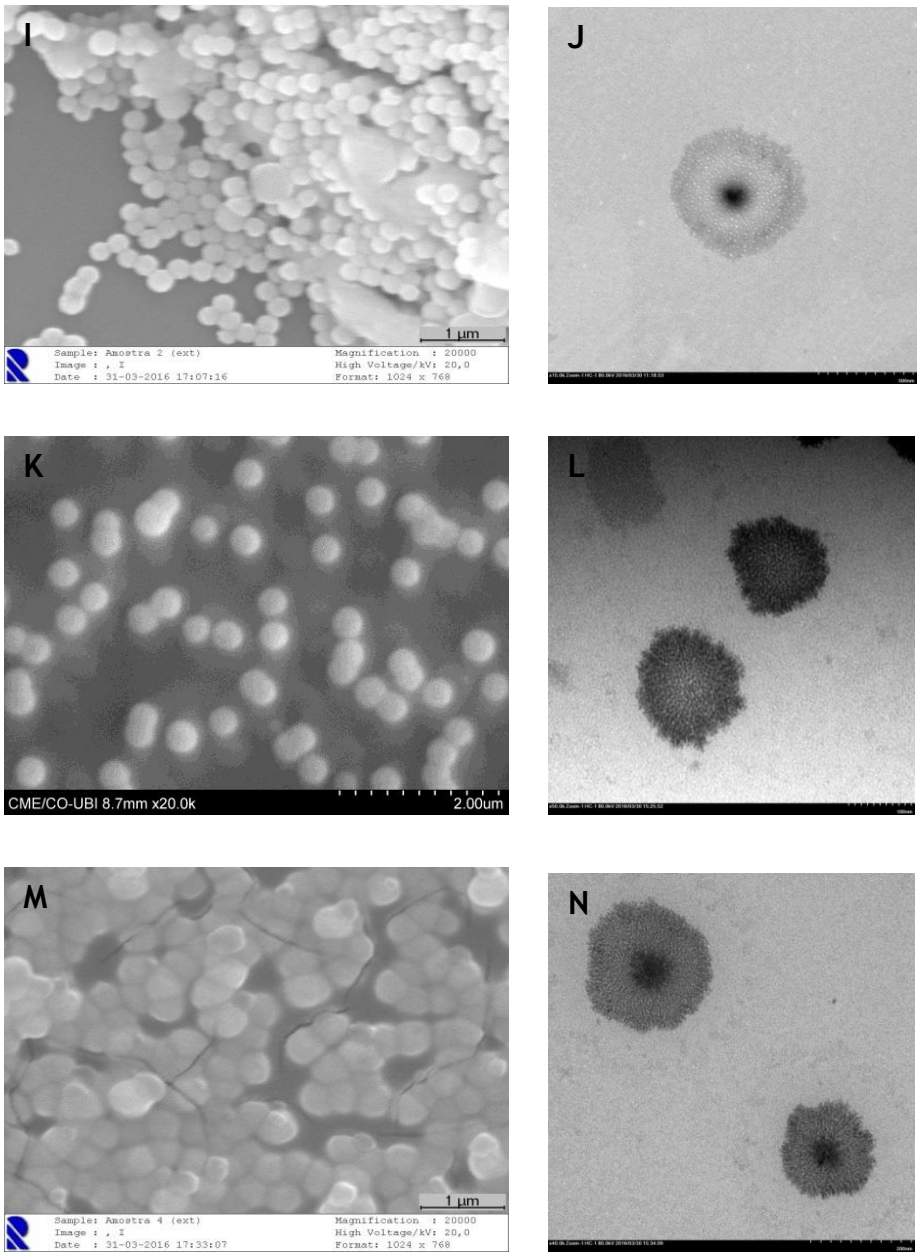

Figure 22 - Morphology of the different system studied. (A and B) Images of pDNA/MgCO3 nanoparticles morphology. (C and D) Images of pDNA/5 mg/mL Gelatin/MgCO3 nanoparticles morphology. (E and F) Images of pDNA/10 mg/mL Gelatin/MgCO3 nanoparticles morphology. (G and H) Images of pDNA/Galactose/MgCO3 nanoparticles morphology. (I and J) Images of pDNA/5 mg/mL Gelatin/Galactose/MgCO3 nanoparticles morphology. (K and L) Images of pDNA/Mannose/MgCO3 nanoparticles morphology. (M and N) Images of pDNA/5 mg/mL Gelatin/Mannose/MgCO3 nanoparticles morphology. All images on the left were obtained by SEM and all images on the right were obtained by TEM.

By analysis of figure 22, the nanoparticles for all the different formulations present a round or oval shape. This is relevant, considering that this morphology allows a quick absorption by the cells membrane, facilitating the nano-carrier internalization.

Two concentrations of gelatin (5 mg/mL and 10 mg/mL) were studied to test the ability of this polymer to reduce the nanoparticles size, but the higher concentration led to the formation of crystals. Thus, 5 mg/mL of gelatin was chosen to formulate the functionalized nanoparticles.

A more detailed analysis of the obtained images revealed that the use of gelatin decreased the size of the nanoparticles, it being in agreement with what was expected [98]. Besides, the functionalization with either mannose or galactose led to the synthesis of nanoparticles with similar sizes.

4.2.6 Nanoparticles size

The morphology influences internalization of the nanoparticles, as well as their size. The mean size of each nanoparticle system studied was determined using the Zetasizer Nano ZS and the obtained values are presented in table 9.

Table 9 - Average size of the different pDNA based nanoparticles. Values were calculated with the data obtained from three independent measurements (mean ± SD, n = 3).

System ($MgCO_3$)	Particle size (nm)
pDNA/5 mg/mL Gelatin	237.4 ± 8.7
pDNA/10 mg/mL Gelatin	213.2 ± 9.0
pDNA/5 mg/mL Mannose	192.6 ± 4.9
pDNA/5 mg/mL Galactose	178.1 ± 4.5
pDNA/5 mg/mL Gelatin/Mannose	142.1 ± 5.7
pDNA/5 mg/mL Gelatin/Galactose	112.8 ± 2.3
pDNA/10 mg/mL Gelatin/Mannose	109.4 ± 9.1
pDNA/10 mg/mL Gelatin/Galactose	99.7 ± 5.9

Is has been described that smaller particles (<300 nm) [126], when complexed with DNA, induce better immune responses than the larger ones. This might be due to the ability of smaller particles to be taken up more readily by APCs. Considering that the studied nano-carriers have sizes between 99.7 nm and 237.4 nm, they have the ideal size. These values are in agreement with the relative sizes from the images obtained with SEM and TEM and are lower than the sizes of $CaCO_3$ nanoparticles (300-500 nm) [95] and similar or lower than the sizes obtained with other formulations [133, 135].

Moreover, it is important to notice that the addition of gelatin causes a reduction on the nanoparticle size, which allows a better absorption and cellular internalization. Besides, the functionalization with mannose or galactose does not lead to the formation of larger

nanoparticles. In summary, all the studied systems present sizes in the nano scale, making them suitable for cellular uptake and thus appropriate for applications within the DNA vaccination.

4.2.7 Zeta (ζ) potential

The ζ potential of each system was measure, as well as the ζ potential of the pDNA and each compound (table 10).

Table 10 - Average zeta potential of the different pDNA based nanoparticles. Values were calculated with the data obtained from three independent measurements (mean ± SD, n = 3).

System ($MgCO_3$)	Zeta Potential (mV)
pDNA	-174.2 ± 9.1
Gelatin	+78.2 ± 5.2
Mannose	+18.4 ± 0.8
Galactose	+37.1 ± 1.3
pDNA/5 mg/mL Gelatin	+65.9 ± 1.5
pDNA/ 10 mg/mL Gelatin	+81.4 ± 3.1
pDNA/5 mg/mL Mannose	+32.1 ± 0.8
pDNA/ 5 mg/mL Galactose	+50 ± 1.7
pDNA/5 mg/mL Gelatin/Mannose	+71.5 ± 6.1
pDNA/5 mg/mL Gelatin/Galactose	+88.9 ± 4.4
pDNA/10 mg/mL Gelatin/Mannose	+82.2 ± 5.1
pDNA/10 mg/mL Gelatin/Galactose	+90.3 ± 6.2

All systems presented positive ζ potential. Besides, it is worth to mention that the presence of gelatin increases the positive charge of the nanoparticles, as it was expected. The positive ζ potential facilitates the future interaction of the nanoparticles with the negatively charged cellular membrane, favoring cell internalization and uptake, therefore enabling a more effective gene transfection.

4.2.8 Transfection studies

Transfection is the process of uptake of nucleic acids, like pDNA, by eukaryotic cells. Thus, the ultimate aim of transfection is to reach the nucleus, where the expression of the therapeutic gene occurs. Besides protection of the pDNA, the goal of the nanoparticles is to mediate and facilitate the cellular uptake.

To evaluate the transfection process, cell live imaging has been performed and applied in fluorescence confocal microscopy. This technique allows for the continuous monitoring of the process for which it was chosen. Cell live imaging was performed through a co-localization

study where the nucleus were stained with Hoechst (blue) and the pDNA within the nanoparticles was previously stained with FITC (green) (figure 23).

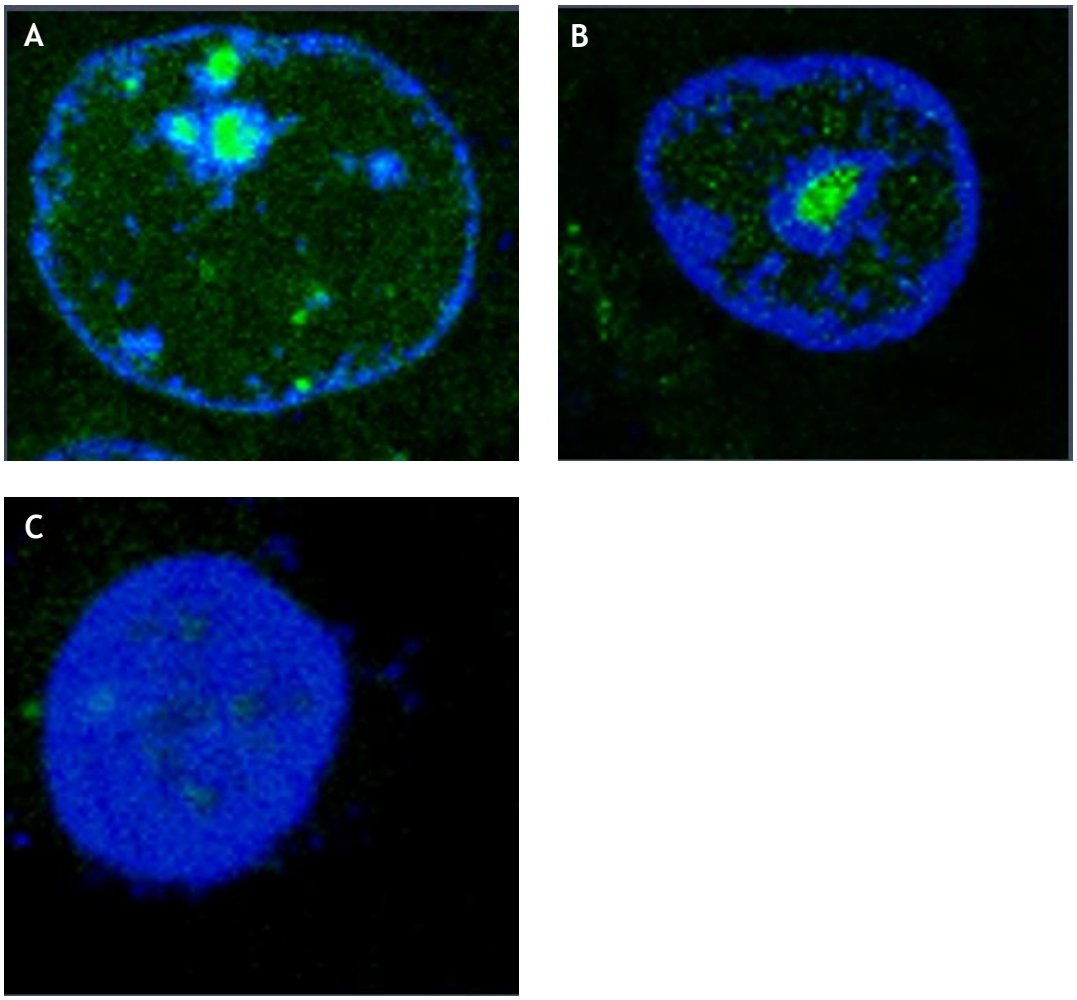

Figure 23 - Transfection ability for the different studied systems. (A) pDNA/Gelatin/$MgCO_3$ nanoparticles transfection. (B) pDNA/Gelatin/Galactose/$MgCO_3$ nanoparticles transfection. (C) pDNA/Gelatin/Mannose/$MgCO_3$ nanoparticles transfection.

Unfortunately, the captured images had some background noise, but still it is possible to observe that the nanoparticles were able to enter the cell and even the nucleus and caused a light blue stain. Although more experiments are required, the images on figure 23 are strong evidence that the nanoparticles were indeed internalized.

Chapter V - Conclusions and future perspectives

Despite the constant and tireless evolution in biotechnology, there are pathologies that remain unaddressed due to the lack of successful treatments, such as HPV infection. DNA vaccination arises as a possible answer to this problem, urging the need to develop efficient purification methods. The use of monolithic chromatography combined with amino acid ligands allows faster separations and increases the selectivity, emerging as a potential way for the sc pDNA purification. After the purification step, it is also crucial to develop systems that can protect and direct the delivery to the target cells, in order to maximize the transfection efficiency and the gene expression of the pDNA molecules.

Hence, the purpose of the present work was to explore different elution strategies and optimize the purification of the sc HPV-16 E6/E7^{MUT} pDNA, using the arginine monolith with spacer arm, in order to fulfil the criteria of the regulatory agencies for therapeutic applications. This work also aimed the formulation and characterization of $MgCO_3$ nanoparticles for *in vitro* transfection.

Initially, a screening of elution gradients were performed to confirm the presence and influence of different functional groups immobilized in epoxy monoliths, namely the electronegative spacer arm and the arginine amino acid ligand, in the pDNA retention. Thereafter, for a complete characterization of the arginine monolith with spacer arm, the dynamic binding capacity was determined, and the value at 10% of breakthrough curve was 2.53 mg/mL, which is lower than the 3.55 mg/mL of the arginine monolith, probably due to the presence of the electronegative spacer arm that promote repulsion by the pDNA. After the preliminary studies of the retention/elution of the different isoforms from a pre-purified sample, different strategies (manipulation of NaCl concentration and/or pH and addition of a competing agent) were explored to obtain the sc pDNA purified from a clarified *E. coli* lysate. After optimizing the conditions, the best strategy was to combine the manipulation of NaCl concentration with the manipulation of pH in the elution buffer (applying a stepwise gradient of 680 mM NaCl in Tris-EDTA, pH 7, 649 mM and 1 M NaCl in Tris-EDTA, pH 7.5), resulting in a sc pDNA purification degree of 93.3% and a recovery yield of 72%. The applicability of this monolith was also evaluated in the purification of the sc pDNA at a preparative scale, with the overloading of the column with a lysate sample. This approach allowed the recovery of 0.83 mg of pDNA/mL of column, with 98.5% of sc pDNA purity (higher than the result obtained at the laboratorial scale). Additionally, all the impurities (RNA, gDNA, proteins and endotoxins) were significantly reduced at acceptable levels by the regulatory agencies, either at laboratorial and preparative scale.

Moreover, a suitable nano-carrier was developed and tested *in vitro*. After adjusting the concentrations of the components, the $MgCO_3$ nanoparticles were functionalized for further targeted delivery. After, the nanoparticles were characterized in terms of encapsulation efficiency (between 60% and 90%), morphology (round shape), size (99.7-237.4 nm) and zeta potential (positive). All these data suggested that the developed nanoparticles were suitable for cellular uptake and thus appropriate for therapeutic applications. Therefore, the *in vitro* studies accompanied with confocal microscopy proved transfection occurrence showing cell internalization, as well as, nucleus targeting of nanoparticles.

In conclusion, it was confirmed that the arginine monolith with spacer arm allowed the sc pDNA purification with a good purity and recovery yield and the $MgCO_3$ nanoparticles proved to be an efficient delivery system, it being a promising strategy for the development of an effective DNA vaccine against HPV infections.

However, the transfection studies must be optimized and immunocytochemistry must be applied in order to evaluate the transfection efficiency of all three developed delivery systems through the analysis of fluorescence intensity differences of the FITC-pDNA. Considering that the DCs are excellent APCs and they have a key role on the activation of the cytotoxic T lymphocytes and the T helper cells, it is important to evaluate the transfection efficiency in these cells. If the functionalization of the nanoparticles by the ligands mannose and galactose enhances the transfection in DCs, then it can be predictable that the *in vitro* systems can perform a targeted delivery to *in vivo* DCs. After selecting the more promising delivery system, *in vitro* transfection studies in DCs should be conducted to evaluate the expression of the E6 and E7 antigenic proteins by immunohistochemistry or western blot. Moreover, *in vivo* studies with mice should be performed to administer the DNA vaccine, using the pDNA encapsulated in the nano-carrier that revealed to be more promising. In addition, to evaluate the activation of immune responses, the quantification of cytotoxic T lymphocytes and T helper cells should be accomplished by flux cytometry.

References

1. Pereira, N., Kucharczyk, K.M., Estes, J.L., Gerber, R.S., Lekovich, J.P., Elias, R.T., Spandorfer, S.D.: Human Papillomavirus Infection, Infertility, and Assisted Reproductive Outcomes. J. Pathog. 2015, 1–8 (2015).
2. Paavonen, J.: Human papillomavirus infection and the development of cervical cancer and related neoplasias. Int. J. Infect. Dis. 11, S3–S9 (2007).
3. Dunne, E.F., Markowitz, L.E., Saraiya, M., Stokley, S., Middleman, A., Unger, E.R., Williams, A., Iskander, J.: CDC grand rounds: Reducing the burden of HPV-associated cancer and disease. MMWR. Morb. Mortal. Wkly. Rep. 63, 69–72 (2014).
4. Hung, C.-F., Monie, A., Alvarez, R.D., Wu, T.-C.: DNA vaccines for cervical cancer: from bench to bedside. Exp Mol Med. 39, 679–689 (2007).
5. Álvarez-Argüelles, M.E., Melón, S., Junquera, M.L., Boga, J.A., Villa, L., Pérez-Castro, S., de Oña, M.: Human Papillomavirus Infection in a Male Population Attending a Sexually Transmitted Infection Service. PLoS One. 8, 1–6 (2013).
6. Doorbar, J.: Molecular biology of human papillomavirus infection and cervical cancer. Clin. Sci. 110, 525–541 (2006).
7. de Villiers, E.-M., Fauquet, C., Broker, T.R., Bernard, H.-U., zur Hausen, H.: Classification of papillomaviruses. Virology. 324, 17–27 (2004).
8. Cheah, P.L., Looi, L.M.: Biology and pathological associations of the human papillomaviruses: a review. Malays. J. Pathol. 20, 1–10 (1998).
9. Zarchi, M.K., Behtash, N., Chiti, Z., Kargar, S.: Cervical Cancer and HPV Vaccines in Developing Countries. Asian Pacific J. Cancer Prev. 10, 969–974 (2009).
10. Nayereh, K.G., Khadem, G.: Preventive and Therapeutic Vaccines against Human Papillomaviruses Associated Cervical Cancers. Iran. J. Basic Med. Sci. 15, 585–601 (2012).
11. Park, T.W., Fujiwara, H., Wright, T.C.: Molecular biology of cervical cancer and its precursors. Cancer. 76, 1902–1913 (1995).
12. Zheng, Z.-M., Baker, C.C.: Papillomavirus genome structure, expression, and post-transcriptional regulation. Front. Biosci. 11, 2286–2302 (2006).
13. Song, D., Li, H., Li, H., Dai, J.: Effect of human papillomavirus infection on the immune system and its role in the course of cervical cancer (Review). Oncol. Lett. 10, 600–606 (2015).
14. McKaig, R.G., Baric, R.S., Olshan, A.F.: Human papillomavirus and head and neck cancer: epidemiology and molecular biology. Head Neck. 20, 250–265 (1998).
15. Motoyama, S., Ladines-llave, C.A., Villanueva, S.L., Maruo, T.: The Role of Human Papilloma Virus in the Molecular Biology of Cervical Carcinogenesis. J. Med. Sci. 50, 9–19 (2004).
16. Yim, E.-K., Park, J.-S.: The role of HPV E6 and E7 oncoproteins in HPV-associated

cervical carcinogenesis. Cancer Res. Treat. 37, 319–324 (2005).
17. Androphy, E.J., Hubbert, N.L., Schiller, J.T., Lowy, D.R.: Identification of the HPV-16 E6 protein from transformed mouse cells and human cervical carcinoma cell lines. EMBO J. 6, 989–992 (1987).
18. McKaig, R.G., Baric, R.S., Olshan, A.F.: Human papillomavirus and head and neck cancer: epidemiology and molecular biology. Head Neck. 20, 250–65 (1998).
19. Howie, H.L., Katzenellenbogen, R.A., Galloway, D.A.: Papillomavirus E6 proteins. Virology. 384, 324–334 (2009).
20. Barbosa, M.S., Lowy, D.R., Schiller, J.T.: Papillomavirus polypeptides E6 and E7 are zinc-binding proteins. J. Virol. 63, 1404–7 (1989).
21. Parrales, A., Iwakuma, T.: Targeting Oncogenic Mutant p53 for Cancer Therapy. Front. Oncol. 5, 1–13 (2015).
22. Sambasivarao, S. V: The papillomavirus E7 proteins. Virology. 445, 138–168 (2013).
23. Phelps, W.C., Münger, K., Yee, C.L., Barnes, J.A., Howley, P.M.: Structure-function analysis of the human papillomavirus type 16 E7 oncoprotein. J. Virol. 66, 2418–27 (1992).
24. Phelps, W.C., Bagchi, S., Barnes, J.A., Raychaudhuri, P., Kraus, V., Munger, K., Howley, P.M., Nevins, J.R.: Analysis of Transactivation by Human Papillomavirus Type-16 E7 and Adenovirus-12s E1a Suggests a Common Mechanism. J Virol. 65, 6922–6930 (1991).
25. Klingelhutz, A.J., Roman, A.: Cellular transformation by human papillomaviruses: Lessons learned by comparing high- and low-risk viruses. Virology. 424, 77–98 (2012).
26. Phelps, W.C., Munger, K., Yee, C.L., Barnes, J.A., Howley, P.M.: Structure-Function Analysis of the Human Papillomavirus Type 16 E7 Oncoprotein. J. Virol. 66, 2418–2427 (1992).
27. Kim, H.J., Lim, S.J., Kwag, H.-L., Kim, H.-J.: The choice of resin-bound ligand affects the structure and immunogenicity of column-purified human papillomavirus type 16 virus-like particles. PLoS One. 7, e35893 (2012).
28. Lin, K., Roosinovich, E., Ma, B., Hung, C.-F., Wu, T.-C.: Therapeutic HPV DNA vaccines. Immunol. Res. 47, 86–112 (2010).
29. Dauner, J.G., Pan, Y., Hildesheim, A., Harro, C., Pinto, L.A.: Characterization of the HPV-specific memory B cell and systemic antibody responses in women receiving an unadjuvanted HPV16 L1 VLP vaccine. Vaccine. 28, 5407–13 (2010).
30. Wang, J.W., Roden, R.B.S.: Virus-like particles for the prevention of human papillomavirus-associated malignancies. Expert Rev. Vaccines. 12, 129–41 (2013).
31. Hung, C.-F., Ma, B., Monie, A., Tsen, S.-W., Wu, T.-C.: Therapeutic human papillomavirus vaccines: Current clinical trials and future directions. Expert Opin. Biol. Ther. 8, 421–439 (2008).
32. Henken, F.E., Oosterhuis, K., Öhlschläger, P., Bosch, L., Hooijberg, E., Haanen, J.B. a G., Steenbergen, R.D.M.: Preclinical safety evaluation of DNA vaccines encoding

modified HPV16 E6 and E7. Vaccine. 30, 4259–66 (2012).
33. Rubanyi, G.M.: The future of human gene therapy. Mol. Aspects Med. 22, 113–142 (2001).
34. Phillips, A.J.: The challenge of gene therapy and DNA delivery. J. Pharm. Pharmacol. 53, 1169–74 (2001).
35. Liu, M.A.: DNA vaccines: a review. J. Intern. Med. 253, 402–410 (2003).
36. Han, Y., Liu, S., Ho, J., Danquah, M.K., Forde, G.M.: Using DNA as a drug—Bioprocessing and delivery strategies. Chem. Eng. Res. Des. 87, 343–348 (2009).
37. Wirth, T., Parker, N., Ylä-Herttuala, S.: History of gene therapy. Gene. 525, 162–9 (2013).
38. Pfeifer, A., Verma, I.M.: GENE THERAPY : Promises and Problems. Genomics. 2, 177–211 (2001).
39. Ibraheem, D., Elaissari, A., Fessi, H.: Gene therapy and DNA delivery systems. Int. J. Pharm. 459, 70–83 (2014).
40. Smith, K.R.: Gene therapy: Theoretical and bioethical concepts. Arch. Med. Res. 34, 247–268 (2003).
41. Gurunathan, S., Klinman, D.M., Seder, R. a: DNA VACCINES : Immunology , Application , and Optimization. Annu. Rev. Immunol. 18, 927–974 (2000).
42. Ghanem, A., Healey, R., Adly, F.G.: Current trends in separation of plasmid DNA vaccines: A review. Anal. Chim. Acta. 760, 1–15 (2013).
43. Coban, C., Kobiyama, K., Jounai, N., Tozuka, M., Ishii, K.J.: DNA vaccines. Hum. Vaccin. Immunother. 9, 2216–2221 (2013).
44. G., Srivastava, I.K., Liu, M.A.: Gene Vaccines. Annu. Intern. Med., vaccines, 138, 550–560 (2003).
45. Monie, A., Tsen, S.-W.D., Hung, C.-F., Wu, T.-C.: Therapeutic HPV DNA vaccines. Expert Rev. Vaccines. 47, 86–112 (2010).
46. Liu, M. a: DNA vaccines: an historical perspective and view to the future. Immunol. Rev. 239, 62–84 (2011).
47. Khan, K.H.: DNA vaccines: Roles against diseases. Germs. 3, 26–35 (2013).
48. Tighe, H., Corr, M., Roman, M., Raz, E.: Gene vaccination: plasmid DNA is more than just a blueprint. Immunol. Today. 19, 89–97 (1998).
49. Han, Y., Liu, S., Ho, J., Danquah, M.K., Forde, G.M.: Using DNA as a drug—Bioprocessing and delivery strategies. Chem. Eng. Res. Des. 87, 343–348 (2009).
50. Pfeifer, A., Verma, I.M.: GENE THERAPY : Promises and Problems. Genomics. 2, 177–211 (2001).
51. Rubanyi, G.M.: The future of human gene therapy. Mol. Aspects Med. 22, 113–142 (2001).
52. Patil, S.D., Rhodes, D.G., Burgess, D.J.: DNA-based therapeutics and DNA delivery systems: a comprehensive review. AAPS J. 7, E61–E77 (2005).
53. Gao, X., Kim, K., Liu, D.: Nonviral Gene Delivery : What We Know and What Is Next.

AAPS J. 9, (2007).

54. Gaspar, V.M., Correia, I.J., Sousa, Â., Silva, F., Paquete, C.M., Queiroz, J. a., Sousa, F.: Nanoparticle mediated delivery of pure P53 supercoiled plasmid DNA for gene therapy. J. Control. Release. 156, 212–222 (2011).
55. M. L. Edelstein. (2016, 20/03/2016). Gene Therapy Clinical Trials Worldwide. Available: http://www.abedia.com/wiley/indications.php
56. Diogo, M.M., Queiroz, J.A., Prazeres, D.M.F.: Chromatography of plasmid DNA. J. Chromatogr. A. 1069, 3–22 (2005).
57. Sousa, F., Prazeres, D.M.F., Queiroz, J.A.: Affinity chromatography approaches to overcome the challenges of purifying plasmid DNA. Trends Biotechnol. 26, 518–525 (2008).
58. Krajnc, N.L., Smrekar, F., Cerne, J., Raspor, P., Modic, M., Krgovic, D., Strancar, A., Podgornik, A.: Purification of large plasmids with methacrylate monolithic columns. J. Sep. Sci. 32, 2682–2690 (2009).
59. Urthaler, J., Buchinger, W., Necina, R.: Improved downstream process for the production of plasmid DNA for gene therapy. Acta Biochim. Pol. 52, 703–711 (2005).
60. Ferreira, G.N., Monteiro, G. a, Prazeres, D.M., Cabral, J.M.: Downstream processing of plasmid DNA for gene therapy and DNA vaccine applications. Trends Biotechnol. 18, 380–388 (2000).
61. Monteiro, G.A., Cabral, J.M.S., Ferreira, G.N.M., Prazeres, D.M.F.: Downstream processing of plasmid DNA for gene therapy and DNA vaccine applications. Trends Biotechnol. 18, 380–388 (2000).
62. Prather, K.J., Sagar, S., Murphy, J., Chartrain, M.: Industrial scale production of plasmid DNA for vaccine and gene therapy: Plasmid design, production, and purification. Enzyme Microb. Technol. 33, 865–883 (2003).
63. Sousa, A., Sousa, F., Queiroz, J.A.: Differential interactions of plasmid DNA, RNA and genomic DNA with amino acid-based affinity matrices. J. Sep. Sci. 33, 2610–2618 (2010).
64. FDA, C.: Guidance for Industry: Considerations for Plasmid DNA Vaccines for Infectious Disease Indications. Biotechnol. Law Rep. 26, 641–648 (2007).
65. Sousa, Â., Sousa, F., Queiroz, J.A.: Advances in chromatographic supports for pharmaceutical-grade plasmid DNA purification. J. Sep. Sci. 00, 1–13 (2012).
66. Sousa, F., Freitas, S., Azzoni, A.R., Prazeres, D.M.F., Queiroz, J.: Selective purification of supercoiled plasmid DNA from clarified cell lysates with a single histidine-agarose chromatography step. Biotechnol. Appl. Biochem. 45, 131–140 (2006).
67. Sousa, A., Sousa, F., Queiroz, J.A.: Differential interactions of plasmid DNA, RNA and genomic DNA with amino acid-based affinity matrices. J. Sep. Sci. 33, 2610–2618 (2010).
68. Pfaunmiller, E.L., Paulemond, M.L., Dupper, C.M., Hage, D.S.: Affinity monolith

chromatography : a review of principles and recent analytical applications. Anal Bioanal Chem 2133–2145 (2013).

69. Sousa, A., Sousa, F., Queiroz, J.A.: Differential interactions of plasmid DNA , RNA and genomic DNA with amino acid- based affinity matrices. J. Sep. Sci. 33, 2610–2618 (2010).
70. Sousa, A., Bicho, D., Tomaz, C.T., Sousa, F., Queiroz, J.A.: Performance of a non-grafted monolithic support for purification of supercoiled plasmid DNA . J. Chromatogr. A. 1218, 1701–1706 (2011).
71. Sousa, A., Sousa, F., Queiroz, J.A.: Impact of lysine-affinity chromatography on supercoiled plasmid DNA purification. J. Chromatogr. B. 879, 3507–3515 (2011).
72. Sousa, F., Prazeres, D.M.F., Queiroz, J.A.: Improvement of transfection efficiency by using supercoiled plasmid DNA purified with arginine affinity chromatography. J. Gene Med. 11, 79–88 (2009).
73. Sousa, A., Tomaz, C.T., Sousa, F., Queiroz, J.A.: Successful application of monolithic innovative technology using a carbonyldiimidazole disk to purify supercoiled plasmid DNA suitable for pharmaceutical applications. J. Chromatogr. A. 1218, 8333–8343 (2011).
74. Sousa, A., Sousa, F., Queiroz, J.A.: Advances in chromatographic supports for pharmaceutical-grade plasmid DNA Journal of Separation Science1–13 (2012).
75. Soares, A., Queiroz, J.A., Sousa, F., Sousa, A.: Purification of human papillomavirus 16 E6/E7 plasmid deoxyribonucleic acid-based vaccine using an arginine modified monolithic support. J. Chromatogr. A. 1320, 72–79 (2013).
76. Bicho, D., Caramelo-Nunes, C., Sousa, A., Sousa, F., Queiroz, J.A., Tomaz, C.T.: Purification of influenza deoxyribonucleic acid-based vaccine using agmatine monolith. J. Chromatogr. B. 1012-1013, 153–161 (2015).
77. Sousa, A., Almeida, A.M., Cernigoj, U., Sousa, F., Queiroz, J.A.: Histamine monolith versatility to purify supercoiled plasmid deoxyribonucleic acid from Escherichia coli lysate. J. Chromatogr. A. 1355, 125–133 (2014).
78. Wang, M., Thanou, M.: Targeting nanoparticles to cancer. Pharmacol. Res. 62, 90–99 (2010).
79. Rao, P.V., Nallappan, D., Madhavi, K., Rahman, S., Jun Wei, L., Gan, S.H.: Phytochemicals and Biogenic Metallic Nanoparticles as Anticancer Agents. Oxid. Med. Cell. Longev. 2016, 1–15 (2016).
80. Vercauteren, D., Rejman, J., Martens, T.F., Demeester, J., De Smedt, S.C., Braeckmans, K.: On the cellular processing of non-viral nanomedicines for nucleic acid delivery: Mechanisms and methods. J. Control. Release. 161, 566–581 (2012).
81. De Jong, W.H., Borm, P.J. a: Drug delivery and nanoparticles:applications and hazards. Int. J. Nanomedicine. 3, 133–149 (2008).
82. Peer, D., Karp, J.M., Hong, S., Farokhzad, O.C., Margalit, R., Langer, R.: Nanocarriers as an emerging platform for cancer therapy. Nat. Nanotechnol. 2, 751–760 (2007).

83. Alberts, B., Johnson, A., Lewis, J., Walter, P., Raff, M., Roberts, K.: Molecular Biology of the Cell 4th Edition: International Student Edition. Routledge (2002).
84. Hart, S.L.: Multifunctional nanocomplexes for gene transfer and gene therapy. Cell Biol. Toxicol. 26, 69–81 (2010).
85. Caracciolo, G., Caminiti, R., Digman, M.A., Gratton, E., Sanchez, S.: Efficient escape from endosomes determines the superior efficiency of multicomponent lipoplexes. J. Phys. Chem. B. 113, 4995–4997 (2009).
86. Varkouhi, A.K., Scholte, M., Storm, G., Haisma, H.J.: Endosomal escape pathways for delivery of biologicals. J. Control. Release. 151, 220–228 (2011).
87. Huang, L., Guo, S.: Nanoparticles escaping RES and endosome: Challenges for siRNA delivery for cancer therapy. J. Nanomater, 2011, 1-12 (2011).
88. He, X., Liu, T., Chen, Y., Cheng, D., Li, X., Xiao, Y., Feng, Y.: Calcium carbonate nanoparticle delivering vascular endothelial growth factor-C siRNA effectively inhibits lymphangiogenesis and growth of gastric cancer in vivo. Cancer Gene Ther. 15, 193–202 (2008).
89. Tseng, W.C., Haselton, F.R., Giorgio, T.D.: Mitosis enhances transgene expression of plasmid delivered by cationic liposomes. Biochim. Biophys. Acta. 1445, 53–64 (1999).
90. Varga, C.M., Wickham, T.J., Lauffenburger, D.A.: Receptor-mediated targeting of gene delivery vectors: Insights from molecular mechanisms for improved vehicle design. Biotechnol. Bioeng. 70, 593–605 (2000).
91. Yih, T.C., Al-Fandi, M.: Engineered nanoparticles as precise drug delivery systems. J. Cell. Biochem. 97, 1184–1190 (2006).
92. Shu, Y., Pi, F., Sharma, A., Rajabi, M.: Stable RNA nanoparticles as potential new generation drugs for cancer therapy. Adv. drug Deliv. 0, 74–89 (2014).
93. Bhakta, G., Shrivastava, A., Maitra, A.: Magnesium phosphate nanoparticles can be efficiently used in vitro and in vivo as non-viral vectors for targeted gene delivery. J. Biomed. Nanotechnol. 5, 106–114 (2009).
94. Liang, P., Zhao, D., Wang, C.Q., Zong, J.Y., Zhuo, R.X., Cheng, S.X.: Facile preparation of heparin/CaCO3/CaP hybrid nano-carriers with controllable size for anticancer drug delivery. Colloids Surfaces B Biointerfaces. 102, 783–788 (2013).
95. Santos, J., Sousa, F., Queiroz, J., Costa, D.: Rhodamine based plasmid DNA nanoparticles for mitochondrial gene therapy. Colloids Surfaces B Biointerfaces. 121, 129–140 (2014).
96. Zhao, D., Liu, C., Zhuo, R., Cheng, S.: Alginate / $CaCO_3$ Hybrid Nanoparticles for Effi cient Codelivery of Antitumor Gene and Drug. Mol. Pharm. (2012).
97. Ma, X., Li, L., Yang, L., Su, C., Wang, K., Jiang, K.: Preparation of hybrid CaCO3–pepsin hemisphere with ordered hierarchical structure and the application for removal of heavy metal ions. J. Cryst. Growth. 338, 272–279 (2012).
98. Samal, S.K., Dash, M., Van Vlierberghe, S., Kaplan, D.L., Chiellini, E., van Blitterswijk, C., Moroni, L., Dubruel, P.: Cationic polymers and their therapeutic potential. Chem.

Soc. Rev. 41, (2012).

99. Münger, K., Phelps, W.C., Bubb, V., Howley, P.M., Schlegel, R.: The E6 and E7 genes of the human papillomavirus type 16 together are necessary and sufficient for transformation of primary human keratinocytes. J. Virol. 63, 4417–21 (1989).
100. J. Sambrook, E.F. Fritsch, T.M.: Molecular Cloning. Cold Spring Harb. Press. New York. (1989).
101. Diogo, M.M., Queiroz, J. a, Monteiro, G. a, Martins, S. a, Ferreira, G.N., Prazeres, D.M.: Purification of a cystic fibrosis plasmid vector for gene therapy using hydrophobic interaction chromatography. Biotechnol. Bioeng. 68, 576–583 (2000).
102. Martins, S.A.M., Prazeres, D.M.F., Cabral, J.M.S., Monteiro, G.A.: Comparison of real-time polymerase chain reaction and hybridization assays for the detection of Escherichia coli genomic DNA in process samples and pharmaceutical-grade plasmid DNA products. Anal. Biochem. 322, 127–129 (2003).
103. Diogo, M.M., Queiroz, J. a, Prazeres, D.M.: Studies on the retention of plasmid DNA and Escherichia coli nucleic acids by hydrophobic interaction chromatography. Bioseparation. 10, 211–220 (2002).
104. Sousa, A., Pereira, P., Sousa, F., Queiroz, J.A.: Binding mechanisms for histamine and agmatine ligands in plasmid deoxyribonucleic acid purifications. J. Chromatogr. A. 1366, 110–119 (2014).
105. Sousa, A., Bicho, D., Tomaz, C.T., Sousa, F., Queiroz, J.A.: Performance of a non-grafted monolithic support for purification of supercoiled plasmid DNA. J. Chromatogr. A. 1218, 1701–1706 (2011).
106. Eon-Duval, A., Burke, G.: Purification of pharmaceutical-grade plasmid DNA by anion-exchange chromatography in an RNase-free process. J. Chromatogr. B Anal. Technol. Biomed. Life Sci. 804, 327–335 (2004).
107. Ongkudon, C.M., Danquah, M.K.: Anion exchange chromatography of 4.2 kbp plasmid based vaccine (pcDNA3F) from alkaline lysed E. coli lysate using amino functionalised polymethacrylate conical monolith. Sep. Purif. Technol. 78, 303–310 (2011).
108. Benčina, M., Podgornik, A., Štrancar, A.: Characterization of methacrylate monoliths for purification of DNA molecules. J. Sep. Sci. 27, 801–810 (2004).
109. Amorim, L.F.A., Sousa, F., Queiroz, J.A., Cruz, C., Sousa, Â.: Screening of l -histidine-based ligands to modify monolithic supports and selectively purify the supercoiled plasmid DNA isoform. J. Mol. Recognit. 28, 349–358 (2015).
110. Pfaunmiller, E.L., Paulemond, M.L., Dupper, C.M., Hage, D.S.: Affinity monolith chromatography: A review of principles and recent analytical applications. Anal. Bioanal. Chem. 405, 2133–2145 (2013).
111. Almeida, A.M., Queiroz, J.A., Sousa, F., Sousa, A.: Optimization of supercoiled HPV-16 E6/E7 plasmid DNA purification with arginine monolith using design of experiments. J. Chromatogr. B. 978-979, 145–150 (2015).
112. Mallik, R., Hage, D.S.: Affinity monolith chromatography. J. Sep. Sci. 29, 1686–1704

(2006).

113. Pereira, P., Sousa, A., Queiroz, J.A., Figueiras, A., Sousa, F.: Pharmaceutical-grade pre-miR-29 purification using an agmatine monolithic support. J. Chromatogr. A. 1368, 173–182 (2014).
114. Sousa, F., Prazeres, D.M.F., Queiroz, J.A.: Binding and elution strategy for improved performance of arginine affinity chromatography in supercoiled plasmid DNA purification. Biomed. Chromatogr. 23, 160–165 (2009).
115. Lee, D., Lee, J., Seok, C.: What stabilizes close arginine pairing in proteins? Phys. Chem. Chem. Phys. 15, 5844–53 (2013).
116. Ongkudon, C.M., Danquah, M.K.: Process optimisation for anion exchange monolithic chromatography of 4.2kbp plasmid vaccine (pcDNA3F). J. Chromatogr. B. 878, 2719–2725 (2010).
117. Giovannini, R., Freitag, R., Tennikova, T.B.: High-performance membrane chromatography of supercoiled plasmid DNA. Anal. Chem. 70, 3348–3354 (1998).
118. Prazeres, D.M.F., Schluep, T., Cooney, C.: Preparative purification of supercoiled plasmid DNA using anion-exchange chromatography. J. Chromatogr. A. 806, 31–45 (1998).
119. Schluep, T., Cooney, C.L.: Purification of plasmids by triplex affinity interaction. Nucleic Acids Res. 26, 4524–4528 (1998).
120. Stadler, J., Lemmens, R., Nyhammar, T.: Plasmid DNA purification. J. Gene Med. 6, 54–66 (2004).
121. Diogo, M.M., Queiroz, J.A., Prazeres, D.M.F.: Purification of plasmid DNA vectors produced in Escherichia coli for gene therapy and DNA vaccination applications. Methods Biotechnol. 18, 165–178 (2005).
122. Ferreira, G.N.M.: Chromatographic approaches in the purification of plasmid DNA for therapy and vaccination. Chem. Eng. Technol. 28, 1285–1294 (2005).
123. Briggs, J., Panfili, P.R.: Quantitation of DNA and protein impurities in biopharmaceuticals. Anal Chem. 63, 850–859 (1991).
124. Butash, K.A., Natarajan, P., Young, A., Fox, D.K.: Reexamination of the effect of endotoxin on cell proliferation and transfection efficiency. Biotechniques. 29, 610–619 (2000).
125. Magalhães, P.O., Lopes, A.M., Mazzola, P.G., Rangel-yagui, C., Penna, T.C. V: Methods of Endotoxin Removal from Biological Preparations : a Review. J Pharm harmaceut Sci. 10, 388–404 (2007).
126. Bhakta, G., Nurcombe, V., Maitra, A., Shrivastava, A.: DNA-encapsulated magnesium phosphate nanoparticles elicit both humoral and cellular immune responses in mice. Results Immunol. (2014).
127. Chowdhury, E.H., Kunou, M., Nagaoka, M., Kundu, A.K., Hoshiba, T., Akaike, T.: High-efficiency gene delivery for expression in mammalian cells by nanoprecipitates of Ca – Mg phosphate. Gene, 341, 77–82 (2004).

128. Jiang, P., Lin, H., Wang, H., Tsai, W., Lin, S., Chien, M., Liang, P., Huang, Y., Liu, D.: Galactosylated liposome as a dendritic cell-targeted mucosal vaccine for inducing protective anti-tumor immunity. Acta Biomater. 11, 356–367 (2015).
129. Kojima, N., Biao, L., Nakayama, T., Ishii, M., Ikehara, Y., Tsujimura, K.: Oligomannose-coated liposomes as a therapeutic antigen-delivery and an adjuvant vehicle for induction of in vivo tumor immunity. J. Control. Release. 129, 26–32 (2008).
130. Jung, S., Kang, S., Yeo, G., Li, H., Jiang, T., Nah, J., Bok, J., Cho, C., Choi, Y.: Targeted Delivery of Vaccine to Dendritic Cells by Chitosan Nanoparticles Conjugated with a Targeting Peptide Ligand Selected by Phage Display Technique. Macromol. Biosci. 15, 395–404 (2015).
131. Wang, H.W., Jiang, P.L., Lin, S.F., Lin, H.J., Ou, K.L., Deng, W.P., Lee, L.W., Huang, Y.Y., Liang, P.H., Liu, D.Z.: Application of galactose-modified liposomes as a potent antigen presenting cell targeted carrier for intranasal immunization. Acta Biomater. 9, 5681–5688 (2013).
132. Jain, S.K., Gupta, Y., Jain, A., Saxena, A.R., Khare, P., Jain, A.: Mannosylated gelatin nanoparticles bearing an anti-HIV drug didanosine for site-specific delivery. Nanomedicine Nanotechnology, Biol. Med. 4, 41–48 (2008).
133. Gaspar, V.M., Sousa, F., Queiroz, J.A., Correia, I.J.: Formulation of chitosan-TPP-pDNA nanocapsules for gene therapy applications. Nanotechnology. 22, 1–12 (2011).
134. Perez, C., Sanchez, A., Putnam, D., Ting, D., Langer, R., Alonso, M.J.: Poly(lactic acid)-poly(ethylene glycol) nanoparticles as new carriers for the delivery of plasmid DNA. J. Control. Release. 75, 211–224 (2001).
135. Gaspar, V.M., Marques, J.G., Sousa, F., Louro, R.O., Queiroz, J. a, Correia, I.J.: Biofunctionalized nanoparticles with pH-responsive and cell penetrating blocks for gene delivery. Nanotechnology. 24, 1–16 (2013).